

Measurement of the relative prompt production rate of χ_{c2} and χ_{c1} in pp collisions at $\sqrt{s} = 7$ TeV

The CMS Collaboration*
CERN, Geneva, Switzerland

Received: 2 October 2012 / Revised: 17 November 2012 / Published online: 14 December 2012
© CERN for the benefit of the CMS collaboration 2012. This article is published with open access at Springerlink.com

Abstract A measurement is presented of the relative prompt production rate of χ_{c2} and χ_{c1} with 4.6 fb^{-1} of data collected by the CMS experiment at the LHC in pp collisions at $\sqrt{s} = 7$ TeV. The two states are measured via their radiative decays $\chi_c \rightarrow J/\psi + \gamma$, with the photon converting into an e^+e^- pair for J/ψ rapidity $|y(J/\psi)| < 1.0$ and photon transverse momentum $p_T(\gamma) > 0.5 \text{ GeV}/c$. The measurement is given for six intervals of $p_T(J/\psi)$ between 7 and 25 GeV/c . The results are compared to theoretical predictions.

1 Introduction

Understanding charmonium production in hadronic collisions is a challenge for quantum chromodynamics (QCD). The J/ψ production cross section measurements at the Tevatron [1, 2] were found to disagree by about a factor of 50 with theoretical color-singlet calculations [3]. Soon after, the CDF experiment reported a χ_{c2}/χ_{c1} cross section ratio that extended up to $p_T(J/\psi) \simeq 10 \text{ GeV}/c$, where p_T is the transverse momentum, and favored χ_{c1} production over χ_{c2} [4]. The cross section ratio was also studied recently at the Large Hadron Collider (LHC) in Ref. [5]. These measurements independently suggest that charmonium production cannot be explained through relatively simple models.

This paper presents a measurement of the prompt χ_{c2}/χ_{c1} cross section ratio by the Compact Muon Solenoid (CMS) experiment at the LHC in pp collisions at a center-of-mass energy of 7 TeV. Prompt refers to the production of χ_c mesons that originate from the primary pp interaction point, as opposed to the ones from the decay of B hadrons. Prompt production includes both directly produced χ_c and also indirectly produced χ_c from the decays of short-lived intermediate states, e.g. the radiative decay of the $\psi(2S)$. The

measurement is based on the reconstruction of the χ_c radiative decays to $J/\psi + \gamma$, with the low transverse momentum photons (less than 5 GeV/c) being detected through their conversion into electron–positron pairs. The analysis uses data collected in 2011, corresponding to a total integrated luminosity of 4.6 fb^{-1} . When estimating acceptance and efficiencies, we assume that the χ_{c2} and χ_{c1} are produced unpolarized, and we supply the correction factors needed to modify the results for several different polarization scenarios.

Due to the extended reach in transverse momentum made possible by the LHC energies, the cross section ratio measurement is expected to discriminate between different predictions, such as those provided by the k_T -factorization [6] and next-to-leading order nonrelativistic QCD (NRQCD) [7] theoretical approaches.

The strength of the ratio measurement is that most theoretical uncertainties cancel, including the quark masses, the value of the strong coupling constant α_s , as well as experimental uncertainties on quantities such as integrated luminosity, trigger efficiencies, and, in part, reconstruction efficiency. Therefore, this ratio can be regarded as an important reference measurement to test the validity of various theoretical quarkonium production models. With this paper, we hope to provide further guidance for future calculations.

2 CMS detector

A detailed description of the CMS apparatus is given in Ref. [8]. Here we provide a short summary of the detectors relevant for this measurement.

The central feature of the CMS apparatus is a superconducting solenoid of 6 m internal diameter. Within the field volume are the silicon pixel and strip tracker, the crystal electromagnetic calorimeter and the brass/scintillator hadron calorimeter. Muons are measured in gas-ionization detectors embedded in the steel return yoke. In addition to

* e-mail: cms-publication-committee-chair@cern.ch

the barrel and endcap detectors, CMS has extensive forward calorimetry.

The inner tracker measures charged particles within the pseudorapidity range $|\eta| < 2.5$, where $\eta = -\ln[\tan(\theta/2)]$, and θ is the polar angle measured from the beam axis. It consists of 1440 silicon pixel and 15 148 silicon strip detector modules. In the central region, modules are arranged in 13 measurement layers. It provides an impact parameter resolution of $\sim 15 \mu\text{m}$.

Muons are measured in the pseudorapidity range $|\eta| < 2.4$, with detection planes made using three technologies: drift tubes, cathode strip chambers, and resistive plate chambers. Matching the muons to the tracks measured in the silicon tracker results in a transverse momentum resolution between 1 and 1.5 %, for p_T values up to 50 GeV/c.

The first level (L1) of the CMS trigger system, composed of custom hardware processors, uses information from the calorimeters and muon detectors to select the most interesting events. The high-level trigger (HLT) processor farm further decreases the event rate from around 100 kHz to around 300 Hz, before data storage. The rate of HLT triggers relevant for this analysis was in the range 5–10 Hz. We analyzed about 60 million such triggers.

3 Experimental method

We select χ_{c1} and χ_{c2} candidates by searching for their radiative decays into the $J/\psi + \gamma$ final state, with the J/ψ decaying into two muons. The χ_{c0} has too small a branching fraction into this final state to perform a useful measurement, but we consider it in the modeling of the signal line-shape. Given the small difference between the J/ψ mass, $3096.916 \pm 0.011 \text{ MeV}/c^2$, and the χ_{c1} and χ_{c2} masses, $3510.66 \pm 0.07 \text{ MeV}/c^2$ and $3556.20 \pm 0.09 \text{ MeV}/c^2$, respectively [9], the detector must be able to reconstruct photons of low transverse momentum. In addition, excellent photon momentum resolution is needed to resolve the two states. In the center-of-mass frame of the χ_c states, the photon has an energy of 390 MeV when emitted by a χ_{c1} and 430 MeV when emitted by a χ_{c2} . This results in most of the photons having a p_T in the laboratory frame smaller than 6 GeV/c. The precision of the cross section ratio measurement depends crucially on the experimental photon energy resolution, which must be good enough to separate the two states. A very accurate measurement of the photon energy is obtained by measuring electron–positron pairs originating from a photon conversion in the beampipe or the inner layers of the silicon tracker. The superior resolution of this approach, compared to a calorimetric energy measurement, comes at the cost of a reduced yield due to the small probability for a conversion to occur in the innermost part of the tracker detector and, more importantly, by the small reconstruction efficiency for low transverse momentum tracks

whose origin is displaced with respect to the beam axis. Nevertheless, because of the high χ_c production cross section at the LHC, the use of conversions leads to the most precise result.

For each $\chi_{c1,2}$ candidate, we evaluate the mass difference $\Delta m = m_{\mu\mu\gamma} - m_{\mu\mu}$ between the dimuon-plus-photon invariant mass, $m_{\mu\mu\gamma}$, and the dimuon invariant mass, $m_{\mu\mu}$. We use the quantity $Q = \Delta m + m_{J/\psi}$, where $m_{J/\psi}$ is the world-average mass of the J/ψ from Ref. [9], as a convenient variable for plotting the invariant-mass distribution. We perform an unbinned maximum-likelihood fit to the Q spectrum to extract the yield of prompt χ_{c1} and χ_{c2} as a function of the transverse momentum of the J/ψ . A correction is applied for the differing acceptances for the two states. Our results are given in terms of the prompt production ratio R_p , defined as

$$R_p \equiv \frac{\sigma(\text{pp} \rightarrow \chi_{c2} + X) \mathcal{B}(\chi_{c2} \rightarrow J/\psi + \gamma)}{\sigma(\text{pp} \rightarrow \chi_{c1} + X) \mathcal{B}(\chi_{c1} \rightarrow J/\psi + \gamma)} = \frac{N_{\chi_{c2}}}{N_{\chi_{c1}}} \cdot \frac{\varepsilon_1}{\varepsilon_2},$$

where $\sigma(\text{pp} \rightarrow \chi_c + X)$ are the χ_c production cross sections, $\mathcal{B}(\chi_c \rightarrow J/\psi + \gamma)$ are the χ_c branching fractions, $N_{\chi_{ci}}$ are the number of candidates of each type obtained from the fit, and $\varepsilon_1/\varepsilon_2$ is the ratio of the efficiencies for the two χ_c states. The branching fractions $\mathcal{B}(\chi_{c1,2} \rightarrow J/\psi + \gamma)$, taken from Ref. [9], are also used to calculate the ratio of production cross sections.

4 Event reconstruction and selection

In order to select χ_c signal events, a dimuon trigger is used to record events containing the decay $J/\psi \rightarrow \mu\mu$. The L1 selection requires two muons without an explicit constraint on their transverse momentum. At the HLT, opposite-charge dimuons are reconstructed and the dimuon rapidity $y(\mu\mu)$ is required to satisfy $|y(\mu\mu)| < 1.0$, while the dimuon p_T must exceed a threshold that increased from 6.5 to 10 GeV/c as the trigger configuration evolved to cope with the instantaneous luminosity increase. Events containing dimuon candidates with invariant mass from 2.95 to 3.25 GeV/c² are recorded. Our data sample consists of events where multiple pp interactions occur. At each bunch crossing, an average of six primary vertices is reconstructed, one of them related to the interaction that produces the χ_c in the final state, the others related to softer collisions (pileup).

In the J/ψ selection, the muon tracks are required to pass the following criteria. They must have at least 11 hits in the tracker, with at least two in the pixel layers, to remove background from decays-in-flight. The χ^2 per degree of freedom of the track fit must be less than 1.8. To remove background from cosmic-ray muons, the tracks must intersect a cylindrical volume of radius 4 cm and total length 70 cm, centered at the nominal interaction point and with its axis parallel to

the beam line. Muon candidate tracks are required to have $p_T > 3.3 \text{ GeV}/c$, $|\eta| \leq 1.3$ and match a well-reconstructed segment in at least one muon detector [10]. Muons with opposite charges are paired. The two muon trajectories are fitted with a common vertex constraint, and events are retained if the fit χ^2 probability is larger than 1 %. If more than one muon pair is found in an event, only the pair with the largest vertex χ^2 probability is selected. For the final χ_{c1} and χ_{c2} selection, a dimuon candidate must have an invariant mass between 3.0 and 3.2 GeV/c^2 and $|\gamma| < 1.0$.

In order to restrict the measurement to the prompt J/ψ signal component, the pseudo-proper decay length of the J/ψ ($\ell_{J/\psi}$), defined as $\ell_{J/\psi} = L_{xy} \cdot m_{J/\psi} / p_T(J/\psi)$, where L_{xy} is the most probable transverse decay length in the laboratory frame [11], is required to be less than 30 μm . In the region $\ell_{J/\psi} < 30 \mu\text{m}$, we estimate, from the observed $\ell_{J/\psi}$ distribution, a contamination of the nonprompt component (originating from the decays of B hadrons) of about 0.7 %, which has a negligible impact on the total systematic uncertainty.

To reconstruct the photon from radiative decays, we use the tracker-based conversion reconstruction described in Refs. [12–14]. We summarize the method here, mentioning the further requirements needed to specialize the conversion reconstruction algorithm to the χ_c case. The algorithm relies on the capability of iterative tracking to efficiently reconstruct displaced and low transverse momentum tracks. Photon conversions are characterized by an electron–positron pair originating from a common vertex. The e^+e^- invariant mass must be consistent with zero within its uncertainties and the two tracks are required to be parallel at the conversion point.

Opposite-sign track pairs are first required to have more than four hits and a normalized χ^2 less than 10. Then the reconstruction algorithm exploits the conversion-pair signature to distinguish between genuine and misidentified background pairs. Information from the calorimeters is not used for conversion reconstruction in our analysis. The primary pp collision vertex associated with the photon conversion, see below, is required to lie outside both track helices. Helices projected onto the transverse plane form circles; we define d_m as the distance between the centers of the two circles minus the sum of their radii. The value of d_m is negative when the two projected trajectories intersect. We require the condition $-0.25 < d_m < 1.0 \text{ cm}$ to be satisfied. From simulation, we have found that most of the electron–positron candidate pair background comes from misreconstructed track pairs originating from the primary vertex. These typically have negative d_m values, thus explaining the asymmetric d_m requirements.

In order to reduce the contribution of misidentified conversions from low-momentum displaced tracks that are artificially propagated back to the silicon tracker, the two candi-

date conversion tracks must have one of their two innermost hits in the same silicon tracker layer.

The distance along the beam line between the extrapolation of each conversion track candidate and the nearest reconstructed event vertex must be less than five times its estimated uncertainty. Moreover, among the two event vertices closest to each track along the beam line, at least one vertex must be in common.

A reconstructed primary vertex is assigned to the reconstructed conversion by projecting the photon momentum onto the beamline and choosing the closest vertex along the beam direction. If the value of the distance is larger than five times its estimated uncertainty, the photon candidate is rejected.

The primary vertex associated with the conversion is required to be compatible with the reconstructed J/ψ vertex. This requirement is fulfilled when the three-dimensional distance between the two vertices is compatible with zero within five standard deviations. Furthermore, a check is made that neither of the two muon tracks used to define the J/ψ vertex is used as one of the conversion track pair.

The e^+e^- track pairs surviving the selection are then fitted to a common vertex with a kinematic vertex fitter that constrains the tracks to be parallel at the vertex in both the transverse and longitudinal planes. The pair is retained if the fit χ^2 probability is greater than 0.05 %. If a track is shared among two or more reconstructed conversions, only the conversion with the larger vertex χ^2 probability is retained.

Only reconstructed conversions with transverse distance of the vertex from the center of the mean pp collision position larger than 1.5 cm are considered. This requirement suppresses backgrounds caused by track pairs originating from the primary event vertex that might mimic a conversion, such as from π^0 Dalitz decay, while retaining photon conversions occurring within the beampipe.

Finally, each conversion candidate is associated with every other conversion candidate in the event, and with any photon reconstructed using calorimeter information. Any pairs of conversions or conversion plus photon with an invariant mass between 0.11 and 0.15 GeV/c^2 , corresponding to a two-standard-deviation window around the π^0 mass, is rejected. We have verified that the π^0 rejection requirement, while effectively reducing the background, does not affect the R_p measurement within its uncertainties.

Converted photon candidates are required to have $p_T > 0.5 \text{ GeV}/c$, while no requirement is imposed on the pseudo-rapidity of the photon.

The distribution of the photon conversion radius for χ_c candidates is shown in Fig. 1. The first peak corresponds to the beampipe and first pixel barrel layer, the second and third peaks correspond to the two outermost pixel layers, while the remaining features at radii larger than 20 cm are due to the four innermost silicon strip layers. The observed distribution of the photon conversion radius is consistent with the

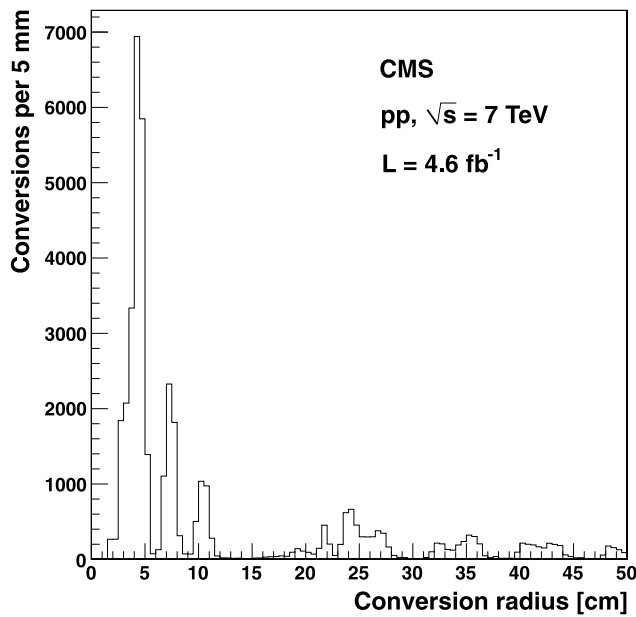


Fig. 1 Distribution of the conversion radius for the χ_c photon candidates

known distribution of material in the tracking volume and with Monte Carlo simulations [14].

5 Acceptance and efficiencies

In the evaluation of R_p , we must take into account the possibility that the geometric acceptance and the photon reconstruction efficiencies are not the same for χ_{c1} and χ_{c2} .

In order to determine the acceptance correction, a Monte Carlo (MC) simulation sample of equal numbers of χ_{c1} and χ_{c2} has been used. This sample was produced using a PYTHIA [15] single-particle simulation in which a χ_{c1} or χ_{c2} is generated with a transverse momentum distribution produced from a parameterized fit to the CMS measured $\psi(2S)$ spectrum [16]. The use of the $\psi(2S)$ spectrum is motivated by the proximity of the $\psi(2S)$ mass to the states under examination. The impact of this choice is discussed in Sect. 7.

Both χ_c states in the simulation are forced to decay to $J/\psi + \gamma$ isotropically in their rest frame, i.e., assuming they are produced unpolarized. We discuss later the impact of this assumption. The decay products are then processed through the full CMS detector simulation, based on GEANT4 [17, 18], and subjected to the trigger emulation and the full event reconstruction. In order to produce the most realistic sample of simulated χ_c decays, digitized signals from MC-simulated inelastic pp events are mixed with those from simulated signal tracks. The number of inelastic events to mix with each signal event is sampled from a Poisson distribution to accurately reproduce the amount of pileup in the data.

The efficiency ratio $\varepsilon_1/\varepsilon_2$ for different J/ψ transverse momentum bins is determined using

$$\frac{\varepsilon_1}{\varepsilon_2} = \frac{N_{\chi_{c1}}^{\text{rec}}}{N_{\chi_{c1}}^{\text{gen}}} \frac{N_{\chi_{c2}}^{\text{rec}}}{N_{\chi_{c2}}^{\text{gen}}},$$

where N^{gen} is the number of χ_c candidates generated in the MC simulation within the kinematic range $|y(J/\psi)| < 1.0$, $p_T(\gamma) > 0.5 \text{ GeV}/c$, and N^{rec} is the number of candidates reconstructed with the selection above. The resulting values are shown in Table 1, where the uncertainties are statistical only and determined from the MC sample assuming binomial distributions. The increasing trend of $\varepsilon_1/\varepsilon_2$ is expected, because $p_T(J/\psi)$ is correlated with the p_T of the photon, and at higher photon p_T our conversion reconstruction efficiency is approximately constant. Therefore, efficiencies for the χ_{c1} and the χ_{c2} are approximately the same at high $p_T(J/\psi)$.

This technique also provides an estimate of the absolute χ_c reconstruction efficiency, which is given by the product of the photon conversion probability, the χ_c selection efficiency, and, most importantly, the conversion reconstruction efficiency, which corresponds to the dominant contribution. This product varies as a function of $p_T(\gamma)$, and goes from 4×10^{-4} at $0.5 \text{ GeV}/c$ to around 10^{-2} at $4 \text{ GeV}/c$, where it saturates.

6 Signal extraction

We extract the numbers of χ_{c1} and χ_{c2} events, $N_{\chi_{c1}}$ and $N_{\chi_{c2}}$, respectively, from the data by performing an unbinned maximum-likelihood fit to the Q spectrum in various ranges of J/ψ transverse momentum.

Because of the small intrinsic width of the χ_c states we are investigating, the observed signal shape is dominated by the experimental resolution. The signal probability density function (PDF) is derived from the MC simulation described in Sect. 5, and is modeled by the superposition of two double-sided Crystal Ball functions [19] for the χ_{c1} and χ_{c2} and a single-sided Crystal Ball function for the χ_{c0} . Each double-sided Crystal Ball function consists of a Gaussian

Table 1 Ratio of efficiencies $\varepsilon_1/\varepsilon_2$ as a function of the J/ψ transverse momentum from MC simulation. The uncertainties are statistical only

$p_T(J/\psi) [\text{GeV}/c]$	$\varepsilon_1/\varepsilon_2$
7–9	0.903 ± 0.023
9–11	0.935 ± 0.019
11–13	0.945 ± 0.021
13–16	0.917 ± 0.022
16–20	0.981 ± 0.031
20–25	1.028 ± 0.049

core with exponential tails on both the high- and low-mass sides. We find this shape to provide an accurate parameterization of the Q spectra derived from MC simulation. When fitting the data, we fix all the parameters of the Crystal Ball function to the values that best fit our MC simulation and use a maximum-likelihood approach to derive $N_{\chi_{c1}}$ and $N_{\chi_{c2}}$, which are the integrals of the PDFs for the two resonances. Because the Q resolution depends on the p_T of the J/ψ , a set of shape parameters is determined for each bin of $p_T(J/\psi)$. Simulation shows that the most important feature of the χ_{c0} signal shape is the low-mass tail due to radiation from the electrons, while the high-mass tail is overwhelmed by the combinatorial background and the low-mass tail of the other resonances. Hence the choice to use a single-sided Crystal Ball function to fit the χ_{c0} mass distribution. Different choices of the χ_{c0} signal parameterization are found to cause variations in the measured R_p values that are well within the quoted systematic uncertainties given below.

The background is modeled by a probability distribution function defined as

$$N_{bkg}(Q) = (Q - q_0)^{\alpha_1} \cdot e^{(Q - q_0) \cdot \beta_1},$$

where α_1 and β_1 are free parameters in the fit, and q_0 is set to $3.2 \text{ GeV}/c^2$.

In Fig. 2 we show the Q distribution for two different ranges, $11 < p_T(J/\psi) < 13 \text{ GeV}/c$ (left) and $16 < p_T(J/\psi) < 20 \text{ GeV}/c$ (right). This procedure is repeated for several ranges in the transverse momentum of the J/ψ in order to extract $N_{\chi_{c1}}$ and $N_{\chi_{c2}}$ in the corresponding bin.

The results are shown in Table 2, where the reported uncertainties are statistical only.

7 Systematic uncertainties

Several types of systematic uncertainty are addressed. In particular, we investigate possible effects that could influence the measurement of the numbers of χ_{c1} and χ_{c2} from

data, the evaluation of $\varepsilon_1/\varepsilon_2$ from the MC simulation, and the derivation of the R_p ratio. In Table 3 the various sources of systematic uncertainties and their contributions to the total uncertainty are summarized. The following subsections describe how the various contributions are evaluated.

7.1 Uncertainty from the mass fit and χ_{c1} and χ_{c2} counting

The measurement of the ratio $N_{\chi_{c2}}/N_{\chi_{c1}}$ could be affected by the choice of the functional form used for the maximum-likelihood fit. The use of an alternative background parameterization, a fourth-order polynomial, results in systematically higher values of the ratio $N_{\chi_{c2}}/N_{\chi_{c1}}$, while keeping the overall fit quality as high as in the default procedure. From the difference in the numbers of signal events using the two background parameterizations, we assign the systematic uncertainty from the background modeling shown in Table 3.

We evaluate the systematic uncertainty related to the parameterization of the signal shape by varying the parameters derived from the MC simulation within their uncertainties. The results fluctuate within 1–3 % in the various transverse momentum ranges. We assign the systematic uncertainties from this source, as shown in Table 3.

The method to disentangle and count the χ_{c1} and χ_{c2} states is validated by using a PYTHIA MC simulation sample of inclusive J/ψ events, including those from χ_c decay, pro-

Table 2 Numbers of χ_{c1} and χ_{c2} events extracted from the maximum-likelihood fit, and the ratio of the two values. Uncertainties are statistical only

$p_T(J/\psi)$ [GeV/c]	$N_{\chi_{c1}}$	$N_{\chi_{c2}}$	$N_{\chi_{c2}}/N_{\chi_{c1}}$
7–9	618 ± 31	315 ± 24	0.510 ± 0.049
9–11	1680 ± 49	788 ± 37	0.469 ± 0.027
11–13	1819 ± 51	819 ± 38	0.451 ± 0.025
13–16	1767 ± 51	851 ± 39	0.482 ± 0.027
16–20	1269 ± 43	487 ± 30	0.384 ± 0.028
20–25	642 ± 31	236 ± 22	0.368 ± 0.040

Fig. 2 The distribution of the variable $Q = m_{\mu\mu\gamma} - m_{\mu\mu} + m_{J/\psi}$ for χ_c candidates with $p_T(J/\psi)$ ranges shown in the figures. The line shows the fit to the data

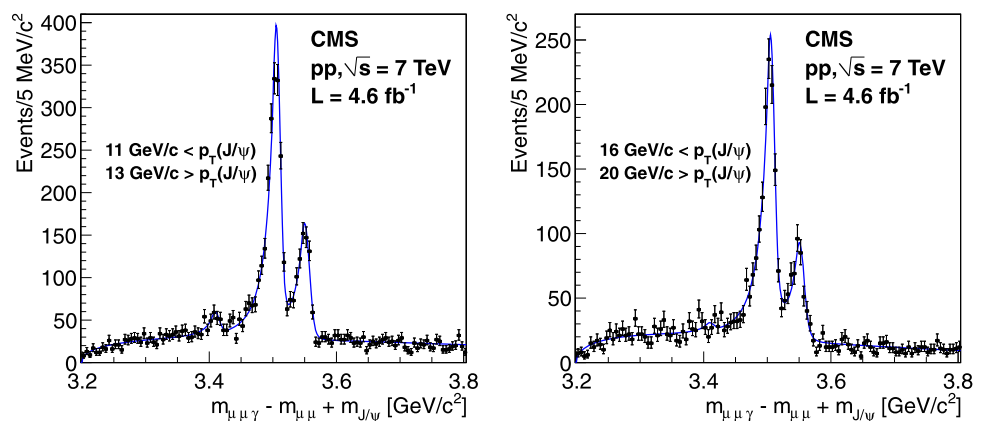


Table 3 Relative systematic uncertainties on R_p for different ranges of J/ψ transverse momentum from different sources and the total uncertainty

$p_T(J/\psi)$ range [GeV/c]	7–9	9–11	11–13	13–16	16–20	20–25
Source of uncertainty	Systematic uncertainty (%)					
Background shape	1.4	1.5	0.9	1.2	1.8	2.4
Signal shape	1.4	3.0	1.1	1.5	1.5	2.3
Simulation sample size	2.6	2.0	2.2	2.4	3.1	4.8
Choice of $p_T(\chi_c)$ spectrum	4.5	3.7	2.9	1.9	0.6	1.1
Total uncertainty	5.5	5.4	3.9	3.6	4.0	5.9

duced in pp collisions and propagated through the full simulation of the detector. The ratio $N_{\chi_{c2}}/N_{\chi_{c1}}$ derived from the fit to the Q distribution of the reconstructed candidates in the simulation is consistent with the actual number of χ_c events contributing to the distribution, within the statistical uncertainty, for all J/ψ momentum ranges. Therefore, we do not assign any further systematic uncertainty in the determination of $N_{\chi_{c2}}/N_{\chi_{c1}}$.

The stability of our analysis as a function of the number of primary vertices in the event has been investigated. The number of χ_c candidates per unit of integrated luminosity, once trigger conditions are taken into account, is found to be independent of the instantaneous luminosity, within the statistical uncertainties. In addition, the measured ratio $N_{\chi_{c2}}/N_{\chi_{c1}}$ is found to be constant as a function of the number of primary vertices in the event, within the statistical uncertainties. Thus, no systematic uncertainty due to pileup is included in the final results.

7.2 Uncertainty in the ratio of efficiencies

The statistical uncertainty in the measurement of $\varepsilon_1/\varepsilon_2$ from the simulation, owing to the finite size of the MC sample, is taken as a systematic uncertainty, as shown in Table 3.

Since the analysis relies on photon conversions, the effect of a possible incorrect simulation of the tracker detector material is estimated. Two modified material scenarios, i.e., special detector geometries prepared for this purpose, in which the total mass of the silicon tracker varies by up to 5 % from the reference geometry, are used to produce new MC simulation samples [20]. With these models, local variations of the radiation length with respect to the reference simulation can be as large as +8 % and −3 %. No significant difference in the ratio of efficiencies is observed and the corresponding systematic uncertainty is taken to be negligible.

Several choices of the generated $p_T(\chi_c)$ spectrum are investigated. In particular, the use of the measured J/ψ spectrum [11] gives values that are compatible with the default $\psi(2S)$ spectrum used for the final result. The choice of the spectrum affects the values of $\varepsilon_1/\varepsilon_2$ only inasmuch as we perform an average measurement in each bin of $p_T(J/\psi)$,

and the size of these bins is finite. We choose to assign a conservative systematic uncertainty by comparing the values of $\varepsilon_1/\varepsilon_2$ obtained with the $\psi(2S)$ spectrum with those obtained in the case where the $p_T(\chi_c)$ spectrum is taken to be constant in each p_T bin. The corresponding systematic uncertainties are given in Table 3.

7.3 χ_c polarization

The polarizations of the χ_{c1} and χ_{c2} are unknown. Efficiencies are estimated under the assumption that the two states are unpolarized. If the χ_c states are polarized, the resulting photon angular distribution and transverse momentum distributions will be affected. This can produce a change in the photon efficiency ratio $\varepsilon_1/\varepsilon_2$.

In order to investigate the impact of different polarization scenarios on the ratio of the efficiencies, we reweight the unpolarized MC distributions to reproduce the theoretical χ_c angular distributions [21, 22] for different χ_c polarizations. We measure the efficiency $\varepsilon_1/\varepsilon_2$ for the χ_{c1} being unpolarized or with helicity $m_{\chi_{c1}} = 0, \pm 1$, in combination with the χ_{c2} being unpolarized or having helicity $m_{\chi_{c2}} = 0, \pm 2$ in both the helicity and Collins–Soper [23] frames. The ratio of efficiencies for the cases involving $m_{\chi_{c2}} = \pm 1$ is between the cases with $m_{\chi_{c2}} = 0$ and $m_{\chi_{c2}} = \pm 2$. Tables 4 and 5 give the resulting $\varepsilon_1/\varepsilon_2$ values for each polarization scenario in different J/ψ transverse momentum bins for the two frames, relative to the value of the ratio for the unpolarized case. These tables, therefore, provide the correction that should be applied to the default value of $\varepsilon_1/\varepsilon_2$ in each polarization scenario and each range of transverse momentum.

7.4 Branching fractions

The measurement of the prompt χ_{c2} to χ_{c1} production cross section ratio is affected by the uncertainties in the branching fractions of the two states into $J/\psi + \gamma$. The quantity that is directly accessible in this analysis is R_p , the product of the ratio of the χ_{c2} to χ_{c1} cross sections and the ratio of the branching fractions.

In order to extract the ratio of the prompt production cross sections, we use the value of 1.76 ± 0.10 for $\mathcal{B}(\chi_{c1} \rightarrow J/\psi + \gamma)/\mathcal{B}(\chi_{c2} \rightarrow J/\psi + \gamma)$ as derived from the branching fractions and associated uncertainties reported in Ref. [9].

Table 4 The efficiency ratio $\varepsilon_1/\varepsilon_2$ for different polarization scenarios in which the χ_{c1} is either unpolarized or has helicity $m_{\chi_{c1}} = 0, \pm 1$ and the χ_{c2} is either unpolarized or has helicity $m_{\chi_{c2}} = 0, \pm 2$ in the helicity frame, relative to the unpolarized case

Polarization scenario ($m_{\chi_{c1}}, m_{\chi_{c2}}$)	$p_T(J/\psi)$ [GeV/c]					
	7–9	9–11	11–13	13–16	16–20	20–25
(Unpolarized, 0)	0.89	0.87	0.85	0.86	0.85	0.86
(Unpolarized, ± 2)	1.20	1.20	1.21	1.20	1.20	1.17
(0, Unpolarized)	0.83	0.84	0.85	0.85	0.85	0.86
(± 1 , Unpolarized)	1.08	1.07	1.07	1.07	1.07	1.07
(0, 0)	0.74	0.73	0.72	0.73	0.72	0.74
(0, ± 2)	1.00	1.01	1.03	1.02	1.02	1.01
(± 1 , 0)	0.95	0.93	0.91	0.97	0.90	0.92
(± 1 , ± 2)	1.29	1.29	1.29	1.28	1.28	1.25

Table 5 The values of $\varepsilon_1/\varepsilon_2$ for different polarization scenarios in the Collins–Soper frame, relative to the unpolarized case

Polarization scenario ($m_{\chi_{c1}}, m_{\chi_{c2}}$)	$p_T(J/\psi)$ [GeV/c]					
	7–9	9–11	11–13	13–16	16–20	20–25
(Unpolarized, 0)	1.04	1.06	1.08	1.07	1.08	1.08
(Unpolarized, ± 2)	0.97	0.95	0.93	0.93	0.92	0.92
(0, Unpolarized)	1.04	1.05	1.06	1.07	1.07	1.06
(± 1 , Unpolarized)	0.98	0.97	0.97	0.96	0.96	0.97
(0, 0)	1.08	1.12	1.14	1.15	1.16	1.14
(0, ± 2)	1.01	0.99	0.98	0.99	0.98	0.98
(± 1 , 0)	1.02	1.03	1.04	1.04	1.04	1.04
(± 1 , ± 2)	0.95	0.92	0.90	0.90	0.89	0.89

8 Results and discussion

The results of the measurement of the ratio R_p and of the ratio of the χ_{c2} to χ_{c1} prompt production cross sections for the kinematic range $p_T(\gamma) > 0.5$ GeV/c and $|y(J/\psi)| < 1.0$ are reported in Tables 6 and 7, respectively, for different ranges of $p_T(J/\psi)$. The first uncertainty is statistical, the second is systematic, and the third comes from the uncertainty in the branching fractions in the measurement of the

cross section ratio. Separate columns are dedicated to the uncertainty derived from the extreme polarization scenarios in the helicity and Collins–Soper frames, by choosing from Tables 4 and 5 the scenarios that give the largest variations relative to the unpolarized case. These correspond to $(m_{\chi_{c1}}, m_{\chi_{c2}}) = (\pm 1, \pm 2)$ and $(m_{\chi_{c1}}, m_{\chi_{c2}}) = (0, 0)$ for both the helicity and Collins–Soper frames. Figure 3 displays the results as a function of the J/ψ transverse momentum for the hypothesis of unpolarized production. The error bars repre-

Table 6 Measurements of $\frac{\sigma(\chi_{c2})\mathcal{B}(\chi_{c2})}{\sigma(\chi_{c1})\mathcal{B}(\chi_{c1})}$ for the given $p_T(J/\psi)$ ranges in the fiducial kinematic region $p_T(\gamma) > 0.5$ GeV/c, $|y(J/\psi)| < 1.0$, assuming unpolarized χ_c production. The first uncertainty is statistical

$p_T(J/\psi)$ [GeV/c]	$\frac{\sigma(\chi_{c2})\mathcal{B}(\chi_{c2})}{\sigma(\chi_{c1})\mathcal{B}(\chi_{c1})}$	HX	CS
7–9	0.460 ± 0.044 (stat.) ± 0.025 (syst.)	+0.136 –0.121	+0.037 –0.023
9–11	0.439 ± 0.025 (stat.) ± 0.024 (syst.)	+0.128 –0.119	+0.052 –0.035
11–13	0.426 ± 0.024 (stat.) ± 0.017 (syst.)	+0.125 –0.117	+0.059 –0.042
13–16	0.442 ± 0.025 (stat.) ± 0.016 (syst.)	+0.125 –0.121	+0.065 –0.044
16–20	0.377 ± 0.028 (stat.) ± 0.015 (syst.)	+0.106 –0.104	+0.059 –0.042
20–25	0.379 ± 0.041 (stat.) ± 0.022 (syst.)	+0.094 –0.097	+0.055 –0.040

and the second is systematic. The last two columns report the additional uncertainties derived from the extreme polarization scenarios in the helicity (HX) and Collins–Soper (CS) frames

Table 7 Measurements of $\sigma(\chi_{c2})/\sigma(\chi_{c1})$ for the given $p_T(J/\psi)$ ranges derived using the branching fractions from Ref. [9], assuming unpolarized χ_c production. The first uncertainty is statistical, the second is systematic, and the third from the branching fraction uncertainties.

$p_T(J/\psi)$ [GeV/c]	$\sigma(\chi_{c2})/\sigma(\chi_{c1})$	HX	CS
7–9	0.811 ± 0.078 (stat.) ± 0.045 (syst.) ± 0.046 (BR)	+0.239 –0.213	+0.066 –0.041
9–11	0.774 ± 0.044 (stat.) ± 0.042 (syst.) ± 0.044 (BR)	+0.225 –0.209	+0.092 –0.061
11–13	0.752 ± 0.042 (stat.) ± 0.029 (syst.) ± 0.043 (BR)	+0.221 –0.207	+0.105 –0.074
13–16	0.78 ± 0.044 (stat.) ± 0.028 (syst.) ± 0.044 (BR)	+0.221 –0.213	+0.115 –0.078
16–20	0.665 ± 0.049 (stat.) ± 0.027 (syst.) ± 0.038 (BR)	+0.187 –0.184	+0.104 –0.074
20–25	0.669 ± 0.072 (stat.) ± 0.039 (syst.) ± 0.038 (BR)	+0.165 –0.172	+0.096 –0.070

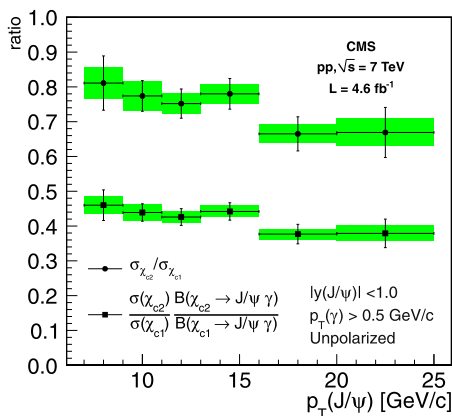


Fig. 3 Ratio of the χ_{c2} to χ_{c1} production cross sections (circles) and ratio of the cross sections times the branching fractions to $J/\psi + \gamma$ (squares) as a function of the J/ψ transverse momentum with the hypothesis of unpolarized production. The error bars correspond to the statistical uncertainties and the band corresponds to the systematic uncertainties. For the cross section ratios, the 5.6 % uncertainty from the branching fractions is not included

sent the statistical uncertainties and the green bands the systematic uncertainties.

Our measurement of the ratio of the prompt χ_{c2} to χ_{c1} cross sections includes both directly produced χ_c mesons and indirectly produced ones from the decays of intermediate states. To convert our result to the ratio of directly produced χ_{c2} to χ_{c1} mesons requires knowledge of the amount of feed-down from all possible short-lived intermediate states that have a decay mode into χ_{c2} or χ_{c1} . The largest known such feed-down contribution comes from the $\psi(2S)$. Using the measured prompt J/ψ and $\psi(2S)$ cross sections in pp collisions at 7 TeV [16], the branching fractions for the decays $\psi(2S) \rightarrow \chi_{c1,2} + \gamma$ [9], and assuming the same fractional χ_c contribution to the total prompt J/ψ production cross section as measured in $p\bar{p}$ collisions at 1.96 TeV [24], we estimate that roughly 5 % of both our

prompt χ_{c1} and χ_{c2} samples come from $\psi(2S)$ decays. The correction in going from the prompt ratio to the direct ratio is about 1 %. In comparing our results with the theoretical predictions described below, we have not attempted to correct for this effect since the uncertainties on the fractions are difficult to estimate, the correction is much smaller than the statistical and systematic uncertainties, and our conclusions on the comparisons with the theoretical predictions would not be altered by a correction of this magnitude.

We compare our results with theoretical predictions derived from the k_T -factorization [6] and NRQCD [7] calculations in Fig. 4. The k_T -factorization approach predicts that both χ_{c1} and χ_{c2} are produced in an almost pure helicity-zero state in the helicity frame. Therefore, in our comparison, we apply the corresponding correction on the ratio of efficiencies from Table 4, amounting to a factor of 0.73, almost independent of p_T . The theoretical calculation is given in the same kinematic range ($p_T(\gamma) > 0.5$ GeV/c, $|y(J/\psi)| < 1.0$) as our measurement. There is no information about the χ_c polarization from the NRQCD calculations, so we use the ratio of efficiencies estimated in the unpolarized case for our comparison. The prediction is given in the kinematic range $p_T(\gamma) > 0$ GeV/c, $|y(J/\psi)| < 1.0$. We use the same MC simulation described in Sect. 5 to derive the small correction factor (ranging from 0.98 to 1.02 depending on p_T , with uncertainties from 1 to 4 %) needed to extrapolate the phase space of our measurement to the one used for the theoretical calculation. The uncertainty in the correction factor stemming from the assumption of the χ_c transverse momentum distribution is added as a systematic uncertainty. The values of R_p after extrapolation are shown in Table 8. The comparison of our measurements with the k_T -factorization and NRQCD predictions are shown in the left and right plots of Fig. 4, respectively. The k_T -factorization prediction agrees well with the trend of R_p versus transverse momentum of the J/ψ , but with a global

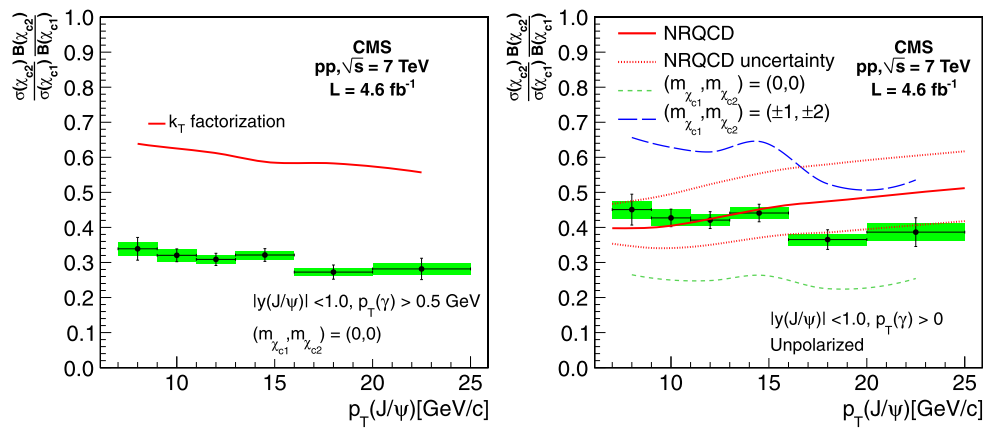


Fig. 4 Comparison of the measured $\frac{\sigma(\chi_{c2})\mathcal{B}(\chi_{c2})}{\sigma(\chi_{c1})\mathcal{B}(\chi_{c1})}$ values with theoretical predictions from the k_T -factorization [6] (left) and NRQCD [7] (right) calculations (solid red lines). The error bars and bands show the experimental statistical and systematic uncertainties, respectively. The measurements in the left plot use an acceptance correction assuming zero helicity for the χ_c , as predicted by the k_T -factorization model. The measurements in the right plot are corrected to match the

kinematic range used in the NRQCD calculation and assume the χ_c are produced unpolarized. The measurements assuming two different extreme polarization scenarios are shown by the long-dashed and short-dashed lines in the plot on the right. The 1-standard-deviation uncertainties in the NRQCD prediction, originating from uncertainties in the color-octet matrix elements, are displayed as the dotted lines

Table 8 Measurements of $\frac{\sigma(\chi_{c2})\mathcal{B}(\chi_{c2})}{\sigma(\chi_{c1})\mathcal{B}(\chi_{c1})}$ for the given $p_T(J/\psi)$ ranges after extrapolating the measurement to the kinematic region $p_T(\gamma) > 0$ and assuming unpolarized χ_c production. The first uncertainty is statistical and the second is systematic. The last column reports the largest variations due changes in the assumed χ_c polarizations

$p_T(J/\psi)$ [GeV/c]	$\frac{\sigma(\chi_{c2})\mathcal{B}(\chi_{c2})}{\sigma(\chi_{c1})\mathcal{B}(\chi_{c1})}$	Polarization
7–9	0.451 ± 0.043 (stat.) ± 0.025 (syst.)	+0.137 –0.153
9–11	0.427 ± 0.024 (stat.) ± 0.023 (syst.)	+0.134 –0.144
11–13	0.421 ± 0.024 (stat.) ± 0.017 (syst.)	+0.133 –0.142
13–16	0.441 ± 0.025 (stat.) ± 0.017 (syst.)	+0.138 –0.143
16–20	0.365 ± 0.027 (stat.) ± 0.016 (syst.)	+0.114 –0.115
20–25	0.387 ± 0.042 (stat.) ± 0.026 (syst.)	+0.109 –0.105

normalization that is higher by about a factor two with respect to our measurement. It is worth noting that this calculation assumes the same wave function for the χ_{c1} and the χ_{c2} . On the other hand, the NRQCD prediction is compatible with our results within the experimental and theoretical uncertainties, though, since predictions for χ_{c1} or χ_{c2} polarizations were not provided, the level of agreement can vary considerably.

A direct comparison of our results with previous measurements, in particular from [4] and [5], is not straightforward, because of the different conditions under which they were carried out. Specifically, there are differences in the kinematical phase space considered and, in the case of [4], in the initial-state colliding beams and center-of-mass energy used. However, with these caveats, a direct comparison shows that the three results are compatible within their uncertainties. In particular, all three results confirm the trend of a decreasing ratio of χ_{c2} to χ_{c1} production cross sections as a function of $p_T(J/\psi)$, under the assumption that the χ_{c2} and χ_{c1} polarizations do not depend on $p_T(J/\psi)$.

9 Summary

Measurements have been presented of the ratio

$$R_p \equiv \frac{\sigma(pp \rightarrow \chi_{c2} + X)\mathcal{B}(\chi_{c2} \rightarrow J/\psi + \gamma)}{\sigma(pp \rightarrow \chi_{c1} + X)\mathcal{B}(\chi_{c1} \rightarrow J/\psi + \gamma)}$$

as a function of the J/ψ transverse momentum up to $p_T(J/\psi) = 25$ GeV/c for the kinematic range $p_T(\gamma) > 0.5$ GeV/c and $|y(J/\psi)| < 1.0$ in pp collisions at $\sqrt{s} = 7$ TeV with a data sample corresponding to an integrated luminosity of 4.6 fb^{-1} . The corresponding values for the ratio of the χ_{c2} to χ_{c1} production cross sections have been determined.

The results have also been shown after extrapolating the photon acceptance down to zero p_T . The effect of several different χ_c polarization scenarios on the photon reconstruction efficiency has been investigated and taken into account in the comparison of the experimental results with two recent theoretical predictions. This is among the most precise measurements of the χ_c production cross section ratio made

in hadron collisions, and extends the explored J/ψ p_T range of previous results. These measurements will provide important input to and constraints on future theoretical calculations of quarkonium production, as recently discussed in [25] for the bottomonium family.

Acknowledgements The authors would like to thank Sergey Baranov for providing theoretical calculations in the k_T -factorization scheme and Kuang-Ta Chao and Yan-Qing Ma for their NRQCD predictions.

We wish to congratulate our colleagues in the CERN accelerator departments for the excellent performance of the LHC machine. We thank the technical and administrative staff at CERN and other CMS institutes. This work was supported by the Austrian Federal Ministry of Science and Research; the Belgium Fonds de la Recherche Scientifique, and Fonds voor Wetenschappelijk Onderzoek; the Brazilian Funding Agencies (CNPq, CAPES, FAPERJ, and FAPESP); the Bulgarian Ministry of Education and Science; CERN; the Chinese Academy of Sciences, Ministry of Science and Technology, and National Natural Science Foundation of China; the Colombian Funding Agency (COLCIENCIAS); the Croatian Ministry of Science, Education and Sport; the Research Promotion Foundation, Cyprus; the Estonian Academy of Sciences and NICPB; the Academy of Finland, Finnish Ministry of Education and Culture, and Helsinki Institute of Physics; the Institut National de Physique Nucléaire et de Physique des Particules / CNRS, and Commissariat à l'Énergie Atomique et aux Énergies Alternatives / CEA, France; the Bundesministerium für Bildung und Forschung, Deutsche Forschungsgemeinschaft, and Helmholtz-Gemeinschaft Deutscher Forschungszentren, Germany; the General Secretariat for Research and Technology, Greece; the National Scientific Research Foundation, and National Office for Research and Technology, Hungary; the Department of Atomic Energy and the Department of Science and Technology, India; the Institute for Studies in Theoretical Physics and Mathematics, Iran; the Science Foundation, Ireland; the Istituto Nazionale di Fisica Nucleare, Italy; the Korean Ministry of Education, Science and Technology and the World Class University program of NRF, Korea; the Lithuanian Academy of Sciences; the Mexican Funding Agencies (CINVESTAV, CONACYT, SEP, and UASLP-FAI); the Ministry of Science and Innovation, New Zealand; the Pakistan Atomic Energy Commission; the Ministry of Science and Higher Education and the National Science Centre, Poland; the Fundação para a Ciência e a Tecnologia, Portugal; JINR (Armenia, Belarus, Georgia, Ukraine, Uzbekistan); the Ministry of Education and Science of the Russian Federation, the Federal Agency of Atomic Energy of the Russian Federation, Russian Academy of Sciences, and the Russian Foundation for Basic Research; the Ministry of Science and Technological Development of Serbia; the Ministerio de Ciencia e Innovación, and Programa Consolider-Ingenio 2010, Spain; the Swiss Funding Agencies (ETH Board, ETH Zurich, PSI, SNF, UniZH, Canton Zurich, and SER); the National Science Council, Taipei; the Scientific and Technical Research Council of Turkey, and Turkish Atomic Energy Authority; the Science and Technology Facilities Council, UK; the US Department of Energy, and the US National Science Foundation.

Individuals have received support from the Marie-Curie programme and the European Research Council (European Union); the Leventis Foundation; the A. P. Sloan Foundation; the Alexander von Humboldt Foundation; the Belgian Federal Science Policy Office; the Fonds pour la Formation à la Recherche dans l'Industrie et dans l'Agriculture (FRIA-Belgium); the Agentschap voor Innovatie door Wetenschap en Technologie (IWT-Belgium); the Council of Science and Industrial Research, India; and the HOMING PLUS programme of Foundation for Polish Science, cofinanced from European Union, Regional Development Fund.

Open Access This article is distributed under the terms of the Creative Commons Attribution License which permits any use, distribution, and reproduction in any medium, provided the original author(s) and the source are credited.

References

1. CDF Collaboration, Inclusive J/ψ , $\psi(2S)$ and b quark production in $p\bar{p}$ collisions at $\sqrt{s} = 1.8$ TeV. Phys. Rev. Lett. **69**, 3704 (1992). doi:[10.1103/PhysRevLett.69.3704](https://doi.org/10.1103/PhysRevLett.69.3704)
2. CDF Collaboration, J/ψ and $\psi(2S)$ production in $p\bar{p}$ collisions at $\sqrt{s} = 1.8$ TeV. Phys. Rev. Lett. **79**, 572 (1997). doi:[10.1103/PhysRevLett.79.572](https://doi.org/10.1103/PhysRevLett.79.572)
3. M. Krämer, Quarkonium production at high-energy colliders. Prog. Part. Nucl. Phys. **47**, 141 (2001). doi:[10.1016/S0146-6410\(01\)00154-5](https://doi.org/10.1016/S0146-6410(01)00154-5). arXiv:[hep-ph/0106120](https://arxiv.org/abs/hep-ph/0106120)
4. CDF Collaboration, Measurement of $\sigma_{\chi_{c2}}\mathcal{B}(\chi_{c2} \rightarrow j/\psi\gamma)/\sigma_{\chi_{c1}}\mathcal{B}(\chi_{c1} \rightarrow j/\psi\gamma)$ in $p\bar{p}$ collisions at $\sqrt{s} = 1.96$ TeV. Phys. Rev. Lett. **98**, 232001 (2007). doi:[10.1103/PhysRevLett.98.232001](https://doi.org/10.1103/PhysRevLett.98.232001). arXiv:[hep-ex/0703028](https://arxiv.org/abs/hep-ex/0703028)
5. LHCb Collaboration, Measurement of the cross-section ratio $\sigma(\chi_{c2})/\sigma(\chi_{c1})$ for prompt χ_c production at $\sqrt{s} = 7$ TeV. Phys. Lett. B **714**, 215 (2012). doi:[10.1016/j.physletb.2012.06.077](https://doi.org/10.1016/j.physletb.2012.06.077). arXiv:[1202.1080](https://arxiv.org/abs/1202.1080)
6. S.P. Baranov, $\sigma(\chi_{c1})/\sigma(\chi_{c2})$ ratio in the k_T -factorization approach. Phys. Rev. D **83**, 034035 (2011). doi:[10.1103/PhysRevD.83.034035](https://doi.org/10.1103/PhysRevD.83.034035)
7. Y.-Q. Ma, K. Wang, K.-T. Chao, QCD radiative corrections to χ_{cJ} production at hadron colliders. Phys. Rev. D **83**, 111503 (2011). doi:[10.1103/PhysRevD.83.111503](https://doi.org/10.1103/PhysRevD.83.111503). arXiv:[1002.3987](https://arxiv.org/abs/1002.3987)
8. CMS Collaboration, The CMS experiment at the CERN LHC. J. Instrum. **3**, S08004 (2008). doi:[10.1088/1748-0221/3/08/S08004](https://doi.org/10.1088/1748-0221/3/08/S08004)
9. J. Beringer et al. (Particle Data Group), Review of particle physics. Phys. Rev. D **86**, 010001 (2012). doi:[10.1103/PhysRevD.86.010001](https://doi.org/10.1103/PhysRevD.86.010001)
10. CMS Collaboration, Performance of CMS muon reconstruction in cosmic-ray events. J. Instrum. **5**, T03022 (2010). doi:[10.1088/1748-0221/5/03/T03022](https://doi.org/10.1088/1748-0221/5/03/T03022). arXiv:[0911.4994](https://arxiv.org/abs/0911.4994)
11. CMS Collaboration, Prompt and non-prompt J/ψ production in pp collisions at $\sqrt{s} = 7$ TeV. Eur. Phys. J. C **71**, 1575 (2011). doi:[10.1140/epjc/s10052-011-1575-8](https://doi.org/10.1140/epjc/s10052-011-1575-8). arXiv:[1011.4193](https://arxiv.org/abs/1011.4193)
12. CMS Collaboration, Tracking and vertexing results from first collisions. CMS physics analysis summary CMS-PAS-TRK-10-001 (2010)
13. CMS Collaboration, CMS tracking performance results from early LHC operation. Eur. Phys. J. C **70**, 1165 (2010). doi:[10.1140/epjc/s10052-010-1491-3](https://doi.org/10.1140/epjc/s10052-010-1491-3). arXiv:[1007.1988](https://arxiv.org/abs/1007.1988)
14. CMS Collaboration, Studies of tracker material in the CMS detector. CMS physics analysis summary CMS-PAS-TRK-10-003 (2010)
15. T. Sjöstrand, S. Mrenna, P. Skands, PYTHIA 6.4 physics and manual. J. High Energy Phys. **05**, 026 (2006). doi:[10.1088/1126-6708/2006/05/026](https://doi.org/10.1088/1126-6708/2006/05/026). arXiv:[hep-ph/0603175](https://arxiv.org/abs/hep-ph/0603175)
16. CMS Collaboration, J/ψ and $\psi(2S)$ production in pp collisions at $\sqrt{s} = 7$ TeV. J. High Energy Phys. **02**, 011 (2012). doi:[10.1007/JHEP02\(2012\)011](https://doi.org/10.1007/JHEP02(2012)011). arXiv:[1111.1557](https://arxiv.org/abs/1111.1557)
17. S. Agostinelli et al., GEANT4—a simulation toolkit. Nucl. Instrum. Methods A **506**, 250 (2003). doi:[10.1016/S0168-9002\(03\)01368-8](https://doi.org/10.1016/S0168-9002(03)01368-8)
18. J. Allison et al., GEANT4 developments and applications. IEEE Trans. Nucl. Sci. **53**, 270 (2006). doi:[10.1109/TNS.2006.869826](https://doi.org/10.1109/TNS.2006.869826)
19. M.J. Oreglia, A study of the reactions $\psi' \rightarrow \gamma\gamma\psi$. PhD thesis, Stanford University, 1980. SLAC Report SLAC-R-236

20. E. Migliore, G. Sguazzoni, Altered scenarios of the CMS Tracker material for systematic uncertainties studies. Technical Report CMS-NOTE-2010-010, CERN (2010)
21. P. Faccioli et al., Determination of χ_c and χ_b polarizations from dilepton angular distributions in radiative decays. Phys. Rev. D **83**, 096001 (2011). doi:[10.1103/PhysRevD.83.096001](https://doi.org/10.1103/PhysRevD.83.096001). [arXiv:1103.4882](https://arxiv.org/abs/1103.4882)
22. HERA-B Collaboration, Production of the charmonium states χ_{c1} and χ_{c2} in proton nucleus interactions at $\sqrt{s} = 41.6$ GeV. Phys. Rev. D **79**, 012001 (2009). doi:[10.1103/PhysRevD.79.012001](https://doi.org/10.1103/PhysRevD.79.012001). [arXiv:0807.2167](https://arxiv.org/abs/0807.2167)
23. J.C. Collins, D.E. Soper, Angular distribution of dileptons in high-energy hadron collisions. Phys. Rev. D **16**, 2219 (1977). doi:[10.1103/PhysRevD.16.2219](https://doi.org/10.1103/PhysRevD.16.2219)
24. CDF Collaboration, Production of J/ψ mesons from χ_c meson decays in $p\bar{p}$ collisions at $\sqrt{s} = 1.8$ TeV. Phys. Rev. Lett. **79**, 578 (1997). doi:[10.1103/PhysRevLett.79.578](https://doi.org/10.1103/PhysRevLett.79.578)
25. A.K. Likhoded, A.V. Luchinsky, S.V. Poslavsky, Production of χ_b mesons at the LHC. Phys. Rev. D **86**, 074027 (2012). doi:[10.1103/PhysRevD.86.074027](https://doi.org/10.1103/PhysRevD.86.074027). [arXiv:1203.4893](https://arxiv.org/abs/1203.4893)

The CMS Collaboration

Yerevan Physics Institute, Yerevan, Armenia

S. Chatrchyan, V. Khachatryan, A.M. Sirunyan, A. Tumasyan

Institut für Hochenergiephysik der OeAW, Wien, Austria

W. Adam, E. Aguilo, T. Bergauer, M. Dragicevic, J. Erö, C. Fabjan¹, M. Friedl, R. Frühwirth¹, V.M. Ghete, J. Hammer, N. Hörmann, J. Hrubec, M. Jeitler¹, W. Kiesenhofer, V. Knünz, M. Krammer¹, I. Krätschmer, D. Liko, I. Mikulec, M. Pernicka[†], B. Rahbaran, C. Rohringer, H. Rohringer, R. Schöfbeck, J. Strauss, A. Taurok, W. Waltenberger, G. Walzel, E. Widl, C.-E. Wulz¹

National Centre for Particle and High Energy Physics, Minsk, Belarus

V. Mossolov, N. Shumeiko, J. Suarez Gonzalez

Universiteit Antwerpen, Antwerpen, Belgium

M. Bansal, S. Bansal, T. Cornelis, E.A. De Wolf, X. Janssen, S. Luyckx, L. Mucibello, S. Ochesanu, B. Roland, R. Rougny, M. Selvaggi, Z. Staykova, H. Van Haevermaet, P. Van Mechelen, N. Van Remortel, A. Van Spilbeeck

Vrije Universiteit Brussel, Brussel, Belgium

F. Blekman, S. Blyweert, J. D'Hondt, R. Gonzalez Suarez, A. Kalogeropoulos, M. Maes, A. Olbrechts, W. Van Doninck, P. Van Mulders, G.P. Van Onsem, I. Vilella

Université Libre de Bruxelles, Bruxelles, Belgium

B. Clerbaux, G. De Lentdecker, V. Dero, A.P.R. Gay, T. Hreus, A. Léonard, P.E. Marage, A. Mohammadi, T. Reis, L. Thomas, G. Vander Marcken, C. Vander Velde, P. Vanlaer, J. Wang

Ghent University, Ghent, Belgium

V. Adler, K. Beernaert, A. Cimmino, S. Costantini, G. Garcia, M. Grunewald, B. Klein, J. Lellouch, A. Marinov, J. McCartin, A.A. Ocampo Rios, D. Ryckbosch, N. Strobbe, F. Thyssen, M. Tytgat, P. Verwilligen, S. Walsh, E. Yazgan, N. Zaganidis

Université Catholique de Louvain, Louvain-la-Neuve, Belgium

S. Basegmez, G. Bruno, R. Castello, L. Ceard, C. Delaere, T. du Pree, D. Favart, L. Forthomme, A. Giammanco², J. Hollar, V. Lemaitre, J. Liao, O. Militaru, C. Nuttens, D. Pagano, A. Pin, K. Piotrkowski, N. Schul, J.M. Vizan Garcia

Université de Mons, Mons, Belgium

N. Beliy, T. Caeberts, E. Daubie, G.H. Hammad

Centro Brasileiro de Pesquisas Fisicas, Rio de Janeiro, Brazil

G.A. Alves, M. Correa Martins Junior, D. De Jesus Damiao, T. Martins, M.E. Pol, M.H.G. Souza

Universidade do Estado do Rio de Janeiro, Rio de Janeiro, Brazil

W.L. Aldá Júnior, W. Carvalho, A. Custódio, E.M. Da Costa, C. De Oliveira Martins, S. Fonseca De Souza, D. Matos Figueiredo, L. Mundim, H. Nogima, V. Oguri, W.L. Prado Da Silva, A. Santoro, L. Soares Jorge, A. Sznajder

Instituto de Fisica Teorica, Universidade Estadual Paulista, Sao Paulo, Brazil

T.S. Anjos³, C.A. Bernardes³, F.A. Dias⁴, T.R. Fernandez Perez Tomei, E.M. Gregores³, C. Lagana, F. Marinho, P.G. Mercadante³, S.F. Novaes, S.S. Padula

Institute for Nuclear Research and Nuclear Energy, Sofia, Bulgaria

V. Genchev⁵, P. Iaydjiev⁵, S. Piperov, M. Rodozov, S. Stoykova, G. Sultanov, V. Tcholakov, R. Trayanov, M. Vutova

University of Sofia, Sofia, Bulgaria

A. Dimitrov, R. Hadjiiska, V. Kozhuharov, L. Litov, B. Pavlov, P. Petkov

Institute of High Energy Physics, Beijing, China

J.G. Bian, G.M. Chen, H.S. Chen, C.H. Jiang, D. Liang, S. Liang, X. Meng, J. Tao, J. Wang, X. Wang, Z. Wang, H. Xiao, M. Xu, J. Zang, Z. Zhang

State Key Lab. of Nucl. Phys. and Tech., Peking University, Beijing, China

C. Asawatangtrakuldee, Y. Ban, Y. Guo, W. Li, S. Liu, Y. Mao, S.J. Qian, H. Teng, D. Wang, L. Zhang, W. Zou

Universidad de Los Andes, Bogota, Colombia

C. Avila, J.P. Gomez, B. Gomez Moreno, A.F. Osorio Oliveros, J.C. Sanabria

Technical University of Split, Split, Croatia

N. Godinovic, D. Lelas, R. Plestina⁶, D. Polic, I. Puljak⁵

University of Split, Split, Croatia

Z. Antunovic, M. Kovac

Institute Rudjer Boskovic, Zagreb, Croatia

V. Brigljevic, S. Duric, K. Kadija, J. Luetic, S. Morovic

University of Cyprus, Nicosia, Cyprus

A. Attikis, M. Galanti, G. Mavromanolakis, J. Mousa, C. Nicolaou, F. Ptochos, P.A. Razis

Charles University, Prague, Czech Republic

M. Finger, M. Finger Jr.

Academy of Scientific Research and Technology of the Arab Republic of Egypt, Egyptian Network of High Energy Physics, Cairo, Egypt

Y. Assran⁷, S. Elgammal⁸, A. Ellithi Kamel⁹, S. Khalil⁸, M.A. Mahmoud¹⁰, A. Radi^{11,12}

National Institute of Chemical Physics and Biophysics, Tallinn, Estonia

M. Kadastik, M. Müntel, M. Raidal, L. Rebane, A. Tiko

Department of Physics, University of Helsinki, Helsinki, Finland

P. Eerola, G. Fedi, M. Voutilainen

Helsinki Institute of Physics, Helsinki, Finland

J. Härkönen, A. Heikkinen, V. Karimäki, R. Kinnunen, M.J. Kortelainen, T. Lampén, K. Lassila-Perini, S. Lehti, T. Lindén, P. Luukka, T. Mäenpää, T. Peltola, E. Tuominen, J. Tuominiemi, E. Tuovinen, D. Ungaro, L. Wendland

Lappeenranta University of Technology, Lappeenranta, Finland

K. Banzuzi, A. Karjalainen, A. Korpela, T. Tuuva

DSM/IRFU, CEA/Saclay, Gif-sur-Yvette, France

M. Besancon, S. Choudhury, M. Dejjardin, D. Denegri, B. Fabbro, J.L. Faure, F. Ferri, S. Ganjour, A. Givernaud, P. Gras, G. Hamel de Monchenault, P. Jarry, E. Locci, J. Malcles, L. Millischer, A. Nayak, J. Rander, A. Rosowsky, I. Shreyber, M. Titov

Laboratoire Leprince-Ringuet, Ecole Polytechnique, IN2P3-CNRS, Palaiseau, France

S. Baffioni, F. Beaudette, L. Benhabib, L. Bianchini, M. Bluj¹³, C. Broutin, P. Busson, C. Charlot, N. Daci, T. Dahms, L. Dobrzynski, R. Granier de Cassagnac, M. Haguenaue, P. Miné, C. Mironov, I.N. Naranjo, M. Nguyen, C. Ochando, P. Paganini, D. Sabes, R. Salerno, Y. Sirois, C. Veelken, A. Zabi

Institut Pluridisciplinaire Hubert Curien, Université de Strasbourg, Université de Haute Alsace Mulhouse, CNRS/IN2P3, Strasbourg, France

J.-L. Agram¹⁴, J. Andrea, D. Bloch, D. Bodin, J.-M. Brom, M. Cardaci, E.C. Chabert, C. Collard, E. Conte¹⁴, F. Drouhin¹⁴, C. Ferro, J.-C. Fontaine¹⁴, D. Gelé, U. Goerlach, P. Juillot, A.-C. Le Bihan, P. Van Hove

Centre de Calcul de l'Institut National de Physique Nucleaire et de Physique des Particules, CNRS/IN2P3, Villeurbanne, France

F. Fassi, D. Mercier

Université de Lyon, Université Claude Bernard Lyon 1, CNRS-IN2P3, Institut de Physique Nucléaire de Lyon, Villeurbanne, France

S. Beauceron, N. Beaupere, O. Bondu, G. Boudoul, J. Chasserat, R. Chierici⁵, D. Contardo, P. Depasse, H. El Mamouni, J. Fay, S. Gascon, M. Gouzevitch, B. Ille, T. Kurca, M. Lethuillier, L. Mirabito, S. Perries, V. Sordini, Y. Tschudi, P. Verdier, S. Viret

Institute of High Energy Physics and Informatization, Tbilisi State University, Tbilisi, Georgia

Z. Tsamalaidze¹⁵

RWTH Aachen University, I. Physikalisches Institut, Aachen, Germany

G. Anagnostou, C. Autermann, S. Beranek, M. Edelhoff, L. Feld, N. Heracleous, O. Hindrichs, R. Jussen, K. Klein, J. Merz, A. Ostapchuk, A. Perieanu, F. Raupach, J. Sammet, S. Schael, D. Sprenger, H. Weber, B. Wittmer, V. Zhukov¹⁶

RWTH Aachen University, III. Physikalisches Institut A, Aachen, Germany

M. Ata, J. Caudron, E. Dietz-Laursonn, D. Duchardt, M. Erdmann, R. Fischer, A. Güth, T. Hebbeker, C. Heidemann, K. Hoepfner, D. Klingebiel, P. Kreuzer, C. Magass, M. Merschmeyer, A. Meyer, M. Olschewski, P. Papacz, H. Pieta, H. Reithler, S.A. Schmitz, L. Sonnenschein, J. Steggemann, D. Teyssier, M. Weber

RWTH Aachen University, III. Physikalisches Institut B, Aachen, Germany

M. Bontenackels, V. Cherepanov, Y. Erdogan, G. Flügge, H. Geenen, M. Geisler, W. Haj Ahmad, F. Hoehle, B. Kargoll, T. Kress, Y. Kuessel, A. Nowack, L. Perchalla, O. Pooth, P. Sauerland, A. Stahl

Deutsches Elektronen-Synchrotron, Hamburg, Germany

M. Aldaya Martin, J. Behr, W. Behrenhoff, U. Behrens, M. Bergholz¹⁷, A. Bethani, K. Borras, A. Burgmeier, A. Cakir, L. Calligaris, A. Campbell, E. Castro, F. Costanza, D. Dammann, C. Diez Pardos, G. Eckerlin, D. Eckstein, G. Flucke, A. Geiser, I. Glushkov, P. Gunnellini, S. Habib, J. Hauk, G. Hellwig, H. Jung, M. Kasemann, P. Katsas, C. Kleinwort, H. Kluge, A. Knutsson, M. Krämer, D. Krücker, E. Kuznetsova, W. Lange, W. Lohmann¹⁷, B. Lutz, R. Mankel, I. Marfin, M. Marienfeld, I.-A. Melzer-Pellmann, A.B. Meyer, J. Mnich, A. Mussgiller, S. Naumann-Emme, J. Olzem, H. Perrey, A. Petrukhin, D. Pitzl, A. Raspereza, P.M. Ribeiro Cipriano, C. Riedl, E. Ron, M. Rosin, J. Salfeld-Nebgen, R. Schmidt¹⁷, T. Schoerner-Sadenius, N. Sen, A. Spiridonov, M. Stein, R. Walsh, C. Wissing

University of Hamburg, Hamburg, Germany

V. Blobel, J. Draeger, H. Enderle, J. Erfle, U. Gebbert, M. Görner, T. Hermanns, R.S. Höing, K. Kaschube, G. Kaussen, H. Kirschenmann, R. Klanner, J. Lange, B. Mura, F. Nowak, T. Peiffer, N. Pietsch, D. Rathjens, C. Sander, H. Schettler, P. Schleper, E. Schlieckau, A. Schmidt, M. Schröder, T. Schum, M. Seidel, V. Sola, H. Stadie, G. Steinbrück, J. Thomsen, L. Vanelderen

Institut für Experimentelle Kernphysik, Karlsruhe, Germany

C. Barth, J. Berger, C. Böser, T. Chwalek, W. De Boer, A. Descroix, A. Dierlamm, M. Feindt, M. Guthoff⁵, C. Hackstein, F. Hartmann, T. Hauth⁵, M. Heinrich, H. Held, K.H. Hoffmann, S. Honc, I. Katkov¹⁶, J.R. Komaragiri, P. Lobelle Pardo, D. Martschei, S. Mueller, Th. Müller, M. Niegel, A. Nürnberg, O. Oberst, A. Oehler, J. Ott, G. Quast, K. Rabbertz, F. Ratnikov, N. Ratnikova, S. Röcker, A. Scheurer, F.-P. Schilling, G. Schott, H.J. Simonis, F.M. Stober, D. Troendle, R. Ulrich, J. Wagner-Kuhr, S. Wayand, T. Weiler, M. Zeise

Institute of Nuclear Physics “Demokritos”, Aghia Paraskevi, Greece

G. Daskalakis, T. Gerasis, S. Kesisoglou, A. Kyriakis, D. Loukas, I. Manolagos, A. Markou, C. Markou, C. Mavrommatis, E. Ntomari

University of Athens, Athens, Greece

L. Gouskos, T.J. Mertzimekis, A. Panagiotou, N. Saoulidou

University of Ioánnina, Ioánnina, Greece

I. Evangelou, C. Foudas, P. Kokkas, N. Manthos, I. Papadopoulos, V. Patras

KFKI Research Institute for Particle and Nuclear Physics, Budapest, Hungary

G. Bencze, C. Hajdu, P. Hidas, D. Horvath¹⁸, F. Sikler, V. Veszpremi, G. Vesztergombi¹⁹

Institute of Nuclear Research ATOMKI, Debrecen, Hungary

N. Beni, S. Czellar, J. Molnar, J. Palinkas, Z. Szillasi

University of Debrecen, Debrecen, Hungary

J. Karancsi, P. Raics, Z.L. Trocsanyi, B. Ujvari

Panjab University, Chandigarh, India

S.B. Beri, V. Bhatnagar, N. Dhingra, R. Gupta, M. Kaur, M.Z. Mehta, N. Nishu, L.K. Saini, A. Sharma, J.B. Singh

University of Delhi, Delhi, India

A. Kumar, A. Kumar, S. Ahuja, A. Bhardwaj, B.C. Choudhary, S. Malhotra, M. Naimuddin, K. Ranjan, V. Sharma, R.K. Shivpuri

Saha Institute of Nuclear Physics, Kolkata, India

S. Banerjee, S. Bhattacharya, S. Dutta, B. Gomber, Sa. Jain, Sh. Jain, R. Khurana, S. Sarkar, M. Sharan

Bhabha Atomic Research Centre, Mumbai, India

A. Abdulsalam, R.K. Choudhury, D. Dutta, S. Kailas, V. Kumar, P. Mehta, A.K. Mohanty⁵, L.M. Pant, P. Shukla

Tata Institute of Fundamental Research - EHEP, Mumbai, India

T. Aziz, S. Ganguly, M. Guchait²⁰, M. Maity²¹, G. Majumder, K. Mazumdar, G.B. Mohanty, B. Parida, K. Sudhakar, N. Wickramage

Tata Institute of Fundamental Research - HECR, Mumbai, India

S. Banerjee, S. Dugad

Institute for Research in Fundamental Sciences (IPM), Tehran, Iran

H. Arfaei, H. Bakhshiansohi²², S.M. Etesami²³, A. Fahim²², M. Hashemi, H. Hesari, A. Jafari²², M. Khakzad, M. Mohammadi Najafabadi, S. Paktinat Mehdiabadi, B. Safarzadeh²⁴, M. Zeinali²³

INFN Sezione di Bari^a, Università di Bari^b, Politecnico di Bari^c, Bari, Italy

M. Abbrescia^{a,b}, L. Barbone^{a,b}, C. Calabria^{a,b,5}, S.S. Chhibra^{a,b}, A. Colaleo^a, D. Creanza^{a,c}, N. De Filippis^{a,c,5}, M. De Palma^{a,b}, L. Fiore^a, G. Iaselli^{a,c}, L. Lusito^{a,b}, G. Maggi^{a,c}, M. Maggi^a, B. Marangelli^{a,b}, S. My^{a,c}, S. Nuzzo^{a,b}, N. Pacifico^{a,b}, A. Pompili^{a,b}, G. Pugliese^{a,c}, G. Selvaggi^{a,b}, L. Silvestris^a, G. Singh^{a,b}, R. Venditti^{a,b}, G. Zito^a

INFN Sezione di Bologna^a, Università di Bologna^b, Bologna, Italy

G. Abbiendi^a, A.C. Benvenuti^a, D. Bonacorsi^{a,b}, S. Braibant-Giacomelli^{a,b}, L. Brigliadori^{a,b}, P. Capiluppi^{a,b}, A. Castro^{a,b}, F.R. Cavallo^a, M. Cuffiani^{a,b}, G.M. Dallavalle^a, F. Fabbri^a, A. Fanfani^{a,b}, D. Fasanella^{a,b,5}, P. Giacomelli^a, C. Grandi^a, L. Guiducci^{a,b}, S. Marcellini^a, G. Masetti^a, M. Meneghelli^{a,b,5}, A. Montanari^a, F.L. Navarria^{a,b}, F. Odorici^a, A. Perrotta^a, F. Primavera^{a,b}, A.M. Rossi^{a,b}, T. Rovelli^{a,b}, G.P. Siroli^{a,b}, R. Travaglini^{a,b}

INFN Sezione di Catania^a, Università di Catania^b, Catania, Italy

S. Albergo^{a,b}, G. Cappello^{a,b}, M. Chiorboli^{a,b}, S. Costa^{a,b}, R. Potenza^{a,b}, A. Tricomi^{a,b}, C. Tuve^{a,b}

INFN Sezione di Firenze^a, Università di Firenze^b, Firenze, Italy

G. Barbagli^a, V. Ciulli^{a,b}, C. Civinini^a, R. D'Alessandro^{a,b}, E. Focardi^{a,b}, S. Frosali^{a,b}, E. Gallo^a, S. Gonzi^{a,b}, M. Meschini^a, S. Paoletti^a, G. Sguazzoni^a, A. Tropiano^a

INFN Laboratori Nazionali di Frascati, Frascati, Italy

L. Benussi, S. Bianco, S. Colafranceschi²⁵, F. Fabbri, D. Piccolo

INFN Sezione di Genova^a, Università di Genova^b, Genova, Italy

P. Fabbriatore^a, R. Musenich^a, S. Tosi^{a,b}

INFN Sezione di Milano-Bicocca^a, Università di Milano-Bicocca^b, Milano, Italy

A. Benaglia^{a,b}, F. De Guio^{a,b}, L. Di Matteo^{a,b,5}, S. Fiorendi^{a,b}, S. Gennai^{a,5}, A. Ghezzi^{a,b}, S. Malvezzi^a, R.A. Manzoni^{a,b}, A. Martelli^{a,b}, A. Massironi^{a,b,5}, D. Menasce^a, L. Moroni^a, M. Paganoni^{a,b}, D. Pedrini^a, S. Ragazzi^{a,b}, N. Redaelli^a, S. Sala^a, T. Tabarelli de Fatis^{a,b}

INFN Sezione di Napoli^a, Università di Napoli "Federico II"^b, Napoli, Italy

S. Buontempo^a, C.A. Carrillo Montoya^a, N. Cavallo^{a,26}, A. De Cosa^{a,b,5}, O. Dogangun^{a,b}, F. Fabozzi^{a,26}, A.O.M. Iorio^a, L. Lista^a, S. Meola^{a,27}, M. Merola^{a,b}, P. Paolucci^{a,5}

INFN Sezione di Padova^a, Università di Padova^b, Università di Trento (Trento)^c, Padova, Italy

P. Azzi^a, N. Bacchetta^{a,5}, D. Bisello^{a,b}, A. Branca^{a,b,5}, R. Carlin^{a,b}, P. Checchia^a, T. Dorigo^a, F. Gasparini^{a,b}, U. Gasparini^{a,b}, A. Gozzelino^a, K. Kanishchev^{a,c}, S. Lacaprara^a, I. Lazzizzera^{a,c}, M. Margoni^{a,b}, A.T. Meneguzzo^{a,b}, J. Pazzini^{a,b}, N. Pozzobon^{a,b}, P. Ronchese^{a,b}, F. Simonetto^{a,b}, E. Torassa^a, M. Tosi^{a,b}, S. Vanini^{a,b}, P. Zotto^{a,b}, A. Zucchetta^{a,b}, G. Zumerle^{a,b}

INFN Sezione di Pavia^a, Università di Pavia^b, Pavia, Italy

M. Gabusi^{a,b}, S.P. Ratti^{a,b}, C. Riccardi^{a,b}, P. Torre^{a,b}, P. Vitulo^{a,b}

INFN Sezione di Perugia^a, Università di Perugia^b, Perugia, Italy

M. Biasini^{a,b}, G.M. Bilei^a, L. Fanò^{a,b}, P. Lariccia^{a,b}, A. Lucaroni^{a,b,5}, G. Mantovani^{a,b}, M. Menichelli^a, A. Nappi^{a,b,†}, F. Romeo^{a,b}, A. Saha^a, A. Santocchia^{a,b}, A. Spiezia^{a,b}, S. Taroni^{a,b}

INFN Sezione di Pisa^a, Università di Pisa^b, Scuola Normale Superiore di Pisa^c, Pisa, Italy

P. Azzurri^{a,c}, G. Bagliesi^a, T. Boccali^a, G. Broccolo^{a,c}, R. Castaldi^a, R.T. D'Agnolo^{a,c}, R. Dell'Orso^a, F. Fiori^{a,b,5}, L. Foà^{a,c}, A. Giassi^a, A. Kraan^a, F. Ligabue^{a,c}, T. Lomtadze^a, L. Martini^{a,28}, A. Messineo^{a,b}, F. Palla^a, A. Rizzi^{a,b}, A.T. Serban^{a,29}, P. Spagnolo^a, P. Squillacioti^{a,5}, R. Tenchini^a, G. Tonelli^{a,b,5}, A. Venturi^a, P.G. Verdini^a

INFN Sezione di Roma^a, Università di Roma^b, Roma, Italy

L. Barone^{a,b}, F. Cavallari^a, D. Del Re^{a,b}, M. Diemoz^a, C. Fanelli^{a,b}, M. Grassi^{a,b,5}, E. Longo^{a,b}, P. Meridiani^{a,5}, F. Micheli^{a,b}, S. Nourbakhsh^{a,b}, G. Organtini^{a,b}, R. Paramatti^a, S. Rahatlou^{a,b}, M. Sigamani^a, L. Soffi^{a,b}

INFN Sezione di Torino^a, Università di Torino^b, Università del Piemonte Orientale (Novara)^c, Torino, Italy

N. Amapane^{a,b}, R. Arcidiacono^{a,c}, S. Argiro^{a,b}, M. Arneodo^{a,c}, C. Biino^a, N. Cartiglia^a, M. Costa^{a,b}, N. Demaria^a, C. Mariotti^{a,5}, S. Maselli^a, E. Migliore^{a,b}, V. Monaco^{a,b}, M. Musich^{a,5}, M.M. Obertino^{a,c}, N. Pastrone^a, M. Pelliccioni^a, A. Potenza^{a,b}, A. Romero^{a,b}, R. Sacchi^{a,b}, A. Solano^{a,b}, A. Staiano^a, E. Usai^{a,b}, A. Vilela Pereira^a

INFN Sezione di Trieste^a, Università di Trieste^b, Trieste, Italy

S. Belforte^a, V. Candelise^{a,b}, F. Cossutti^a, G. Della Ricca^{a,b}, B. Gobbo^a, M. Marone^{a,b,5}, D. Montanino^{a,b,5}, A. Penzo^a, A. Schizzi^{a,b}

Kangwon National University, Chunchon, Korea

S.G. Heo, T.Y. Kim, S.K. Nam

Kyungpook National University, Daegu, Korea

S. Chang, D.H. Kim, G.N. Kim, D.J. Kong, H. Park, S.R. Ro, D.C. Son, T. Son

Chonnam National University, Institute for Universe and Elementary Particles, Kwangju, Korea

J.Y. Kim, Z.J. Kim, S. Song

Korea University, Seoul, Korea

S. Choi, D. Gyun, B. Hong, M. Jo, H. Kim, T.J. Kim, K.S. Lee, D.H. Moon, S.K. Park

University of Seoul, Seoul, Korea

M. Choi, J.H. Kim, C. Park, I.C. Park, S. Park, G. Ryu

Sungkyunkwan University, Suwon, Korea

Y. Cho, Y. Choi, Y.K. Choi, J. Goh, M.S. Kim, E. Kwon, B. Lee, J. Lee, S. Lee, H. Seo, I. Yu

Vilnius University, Vilnius, Lithuania

M.J. Bilinskas, I. Grigelionis, M. Janulis, A. Juodagalvis

Centro de Investigacion y de Estudios Avanzados del IPN, Mexico City, Mexico

H. Castilla-Valdez, E. De La Cruz-Burelo, I. Heredia-de La Cruz, R. Lopez-Fernandez, R. Magaña Villalba, J. Martínez-Ortega, A. Sánchez-Hernández, L.M. Villaseñor-Cendejas

Universidad Iberoamericana, Mexico City, Mexico

S. Carrillo Moreno, F. Vazquez Valencia

Benemerita Universidad Autonoma de Puebla, Puebla, Mexico

H.A. Salazar Ibarguen

Universidad Autónoma de San Luis Potosí, San Luis Potosí, Mexico

E. Casimiro Linares, A. Morelos Pineda, M.A. Reyes-Santos

University of Auckland, Auckland, New Zealand

D. Krofcheck

University of Canterbury, Christchurch, New Zealand

A.J. Bell, P.H. Butler, R. Doesburg, S. Reucroft, H. Silverwood

National Centre for Physics, Quaid-I-Azam University, Islamabad, Pakistan

M. Ahmad, M.H. Ansari, M.I. Asghar, H.R. Hoorani, S. Khalid, W.A. Khan, T. Khurshid, S. Qazi, M.A. Shah, M. Shoaib

National Centre for Nuclear Research, Swierk, Poland

H. Bialkowska, B. Boimska, T. Frueboes, R. Gokieli, M. Górski, M. Kazana, K. Nawrocki, K. Romanowska-Rybinska, M. Szleper, G. Wrochna, P. Zalewski

Institute of Experimental Physics, Faculty of Physics, University of Warsaw, Warsaw, Poland

G. Brona, K. Bunkowski, M. Cwiok, W. Dominik, K. Doroba, A. Kalinowski, M. Konecki, J. Krolikowski

Laboratório de Instrumentação e Física Experimental de Partículas, Lisboa, Portugal

N. Almeida, P. Bargassa, A. David, P. Faccioli, P.G. Ferreira Parracho, M. Gallinaro, J. Seixas, J. Varela, P. Vischia

Joint Institute for Nuclear Research, Dubna, Russia

I. Belotelov, P. Bunin, M. Gavrilenko, I. Golutvin, I. Gorbunov, A. Kamenev, V. Karjavin, G. Kozlov, A. Lanev, A. Malakhov, P. Moisenz, V. Palichik, V. Perelygin, S. Shmatov, V. Smirnov, A. Volodko, A. Zarubin

Petersburg Nuclear Physics Institute, Gatchina (St. Petersburg), Russia

S. Evstyukhin, V. Golovtsov, Y. Ivanov, V. Kim, P. Levchenko, V. Murzin, V. Oreshkin, I. Smirnov, V. Sulimov, L. Uvarov, S. Vavilov, A. Vorobyev, An. Vorobyev

Institute for Nuclear Research, Moscow, Russia

Yu. Andreev, A. Dermenev, S. Gninenko, N. Golubev, M. Kirsanov, N. Krasnikov, V. Matveev, A. Pashenkov, D. Tisov, A. Toropin

Institute for Theoretical and Experimental Physics, Moscow, Russia

V. Epshteyn, M. Erofeeva, V. Gavrilo, M. Kossov, N. Lychkovskaya, V. Popov, G. Safronov, S. Semenov, V. Stolin, E. Vlasov, A. Zhokin

Moscow State University, Moscow, RussiaA. Belyaev, E. Boos, M. Dubinin⁴, L. Dudko, A. Ershov, A. Gribushin, V. Klyukhin, O. Kodolova, I. Lokhtin, A. Markina, S. Obraztsov, M. Perfilov, S. Petrushanko, A. Popov, L. Sarycheva[†], V. Savrin, A. Snigirev**P.N. Lebedev Physical Institute, Moscow, Russia**

V. Andreev, M. Azarkin, I. Dremin, M. Kirakosyan, A. Leonidov, G. Mesyats, S.V. Rusakov, A. Vinogradov

State Research Center of Russian Federation, Institute for High Energy Physics, Protvino, RussiaI. Azhgirey, I. Bayshev, S. Bitioukov, V. Grishin⁵, V. Kachanov, D. Konstantinov, V. Krychkin, V. Petrov, R. Ryutin, A. Sobol, L. Tourtchanovitch, S. Troshin, N. Tyurin, A. Uzunian, A. Volkov**University of Belgrade, Faculty of Physics and Vinca Institute of Nuclear Sciences, Belgrade, Serbia**P. Adzic³⁰, M. Djordjevic, M. Ekmedzic, D. Krpic³⁰, J. Milosevic**Centro de Investigaciones Energéticas Medioambientales y Tecnológicas (CIEMAT), Madrid, Spain**

M. Aguilar-Benitez, J. Alcaraz Maestre, P. Arce, C. Battilana, E. Calvo, M. Cerrada, M. Chamizo Llatas, N. Colino, B. De La Cruz, A. Delgado Peris, D. Domínguez Vázquez, C. Fernandez Bedoya, J.P. Fernández Ramos, A. Ferrando, J. Flix, M.C. Fouz, P. Garcia-Abia, O. Gonzalez Lopez, S. Goy Lopez, J.M. Hernandez, M.I. Josa, G. Merino, J. Puerta Pelayo, A. Quintario Olmeda, I. Redondo, L. Romero, J. Santaolalla, M.S. Soares, C. Willmott

Universidad Autónoma de Madrid, Madrid, Spain

C. Albajar, G. Codispoti, J.F. de Trocóniz

Universidad de Oviedo, Oviedo, Spain

H. Brun, J. Cuevas, J. Fernandez Menendez, S. Folgueras, I. Gonzalez Caballero, L. Lloret Iglesias, J. Piedra Gomez

Instituto de Física de Cantabria (IFCA), CSIC-Universidad de Cantabria, Santander, Spain

J.A. Brochero Cifuentes, I.J. Cabrillo, A. Calderon, S.H. Chuang, J. Duarte Campderros, M. Felcini³¹, M. Fernandez, G. Gomez, J. Gonzalez Sanchez, A. Graziano, C. Jorda, A. Lopez Virto, J. Marco, R. Marco, C. Martinez Rivero, F. Matorras, F.J. Munoz Sanchez, T. Rodrigo, A.Y. Rodríguez-Marrero, A. Ruiz-Jimeno, L. Scodellaro, I. Vila, R. Vilar Cortabitarte

CERN, European Organization for Nuclear Research, Geneva, Switzerland

D. Abbaneo, E. Auffray, G. Auzinger, M. Bachtis, P. Baillon, A.H. Ball, D. Barney, J.F. Benitez, C. Bernet⁶, G. Bianchi, P. Bloch, A. Bocci, A. Bonato, C. Botta, H. Breuker, T. Camporesi, G. Cerminara, T. Christiansen, J.A. Coarasa Perez, D. D'Enterria, A. Dabrowski, A. De Roeck, S. Di Guida, M. Dobson, N. Dupont-Sagorin, A. Elliott-Peisert, B. Frisch, W. Funk, G. Georgiou, M. Giffels, D. Gigi, K. Gill, D. Giordano, M. Giunta, F. Glege, R. Gomez-Reino Garrido, P. Govoni, S. Gowdy, R. Guida, M. Hansen, P. Harris, C. Hartl, J. Harvey, B. Hegner, A. Hinzmann, V. Innocente, P. Janot, K. Kaadze, E. Karavakis, K. Kousouris, P. Lecoq, Y.-J. Lee, P. Lenzi, C. Lourenço, N. Magini, T. Mäki, M. Malberti, L. Malgeri, M. Mannelli, L. Masetti, F. Meijers, S. Mersi, E. Meschi, R. Moser, M.U. Mozer, M. Mulders, P. Musella, E. Nesvold, T. Orimoto, L. Orsini, E. Palencia Cortezon, E. Perez, L. Perrozzi, A. Petrilli, A. Pfeiffer, M. Pierini, M. Pimiä, D. Piparo, G. Polese, L. Quertenmont, A. Racz, W. Reece, J. Rodrigues Antunes, G. Rolandi³², C. Rovelli³³, M. Rovere, H. Sakulin, F. Santanastasio, C. Schäfer, C. Schwick, I. Segoni, S. Sekmen, A. Sharma, P. Siegrist, P. Silva, M. Simon, P. Sphicas³⁴, D. Spiga, A. Tsiros, G.I. Veres¹⁹, J.R. Vlimant, H.K. Wöhri, S.D. Worm³⁵, W.D. Zeuner

Paul Scherrer Institut, Villigen, Switzerland

W. Bertl, K. Deiters, W. Erdmann, K. Gabathuler, R. Horisberger, Q. Ingram, H.C. Kaestli, S. König, D. Kotlinski, U. Langenegger, F. Meier, D. Renker, T. Rohe, J. Sibille³⁶

Institute for Particle Physics, ETH Zurich, Zurich, Switzerland

L. Bäni, P. Bortignon, M.A. Buchmann, B. Casal, N. Chanon, A. Deisher, G. Dissertori, M. Dittmar, M. Donegà, M. Dünser, J. Eugster, K. Freudenreich, C. Grab, D. Hits, P. Lecomte, W. Lustermann, A.C. Marini, P. Martinez Ruiz del Arbol, N. Mohr, F. Moortgat, C. Nägeli³⁷, P. Nef, F. Nessi-Tedaldi, F. Pandolfi, L. Pape, F. Pauss, M. Peruzzi, F.J. Ronga, M. Rossini, L. Sala, A.K. Sanchez, A. Starodumov³⁸, B. Stieger, M. Takahashi, L. Tauscher[†], A. Thea, K. Theofilatos, D. Treille, C. Urscheler, R. Wallny, H.A. Weber, L. Wehrli

Universität Zürich, Zurich, Switzerland

C. AMSler, V. Chiochia, S. De Visscher, C. Favaro, M. Ivova Rikova, B. Millan Mejias, P. Otiougova, P. Robmann, H. Snoek, S. Tuppatti, M. Verzett

National Central University, Chung-Li, Taiwan

Y.H. Chang, K.H. Chen, C.M. Kuo, S.W. Li, W. Lin, Z.K. Liu, Y.J. Lu, D. Mekterovic, A.P. Singh, R. Volpe, S.S. Yu

National Taiwan University (NTU), Taipei, Taiwan

P. Bartalini, P. Chang, Y.H. Chang, Y.W. Chang, Y. Chao, K.F. Chen, C. Dietz, U. Grundler, W.-S. Hou, Y. Hsiung, K.Y. Kao, Y.J. Lei, R.-S. Lu, D. Majumder, E. Petrakou, X. Shi, J.G. Shiu, Y.M. Tzeng, X. Wan, M. Wang

Cukurova University, Adana, Turkey

A. Adiguzel, M.N. Bakirci³⁹, S. Cerci⁴⁰, C. Dozen, I. Dumanoglu, E. Eskut, S. Girgis, G. Gokbulut, E. Gurpinar, I. Hos, E.E. Kangal, T. Karaman, G. Karapinar⁴¹, A. Kayis Topaksu, G. Onengut, K. Ozdemir, S. Ozturk⁴², A. Polatoz, K. Sogut⁴³, D. Sunar Cerci⁴⁰, B. Tali⁴⁰, H. Topakli³⁹, L.N. Vergili, M. Vergili

Middle East Technical University, Physics Department, Ankara, Turkey

I.V. Akin, T. Aliev, B. Bilin, S. Bilmis, M. Deniz, H. Gamsizkan, A.M. Guler, K. Ocalan, A. Ozpineci, M. Serin, R. Sever, U.E. Surat, M. Yalvac, E. Yildirim, M. Zeyrek

Bogazici University, Istanbul, Turkey

E. Gülmez, B. Isildak⁴⁴, M. Kaya⁴⁵, O. Kaya⁴⁵, S. Ozkorucuklu⁴⁶, N. Sonmez⁴⁷

Istanbul Technical University, Istanbul, Turkey

K. Cankocak

National Scientific Center, Kharkov Institute of Physics and Technology, Kharkov, Ukraine

L. Levchuk

University of Bristol, Bristol, United Kingdom

F. Bostock, J.J. Brooke, E. Clement, D. Cussans, H. Flacher, R. Frazier, J. Goldstein, M. Grimes, G.P. Heath, H.F. Heath, L. Kreczko, S. Metson, D.M. Newbold³⁵, K. Nirunpong, A. Poll, S. Senkin, V.J. Smith, T. Williams

Rutherford Appleton Laboratory, Didcot, United Kingdom

L. Basso⁴⁸, K.W. Bell, A. Belyaev⁴⁸, C. Brew, R.M. Brown, D.J.A. Cockerill, J.A. Coughlan, K. Harder, S. Harper, J. Jackson, B.W. Kennedy, E. Olaiya, D. Petyt, B.C. Radburn-Smith, C.H. Shepherd-Themistocleous, I.R. Tomalin, W.J. Womersley

Imperial College, London, United Kingdom

R. Bainbridge, G. Ball, R. Beuselinck, O. Buchmuller, D. Colling, N. Cripps, M. Cutajar, P. Dauncey, G. Davies, M. Della Negra, W. Ferguson, J. Fulcher, D. Futyan, A. Gilbert, A. Guneratne Bryer, G. Hall, Z. Hatherell, J. Hays, G. Iles, M. Jarvis, G. Karapostoli, L. Lyons, A.-M. Magnan, J. Marrouche, B. Mathias, R. Nandi, J. Nash, A. Nikitenko³⁸, A. Papageorgiou, J. Pela, M. Pesaresi, K. Petridis, M. Pioppi⁴⁹, D.M. Raymond, S. Rogerson, A. Rose, M.J. Ryan, C. Seez, P. Sharp[†], A. Sparrow, M. Stoye, A. Tapper, M. Vazquez Acosta, T. Virdee, S. Wakefield, N. Wardle, T. Whyntie

Brunel University, Uxbridge, United Kingdom

M. Chadwick, J.E. Cole, P.R. Hobson, A. Khan, P. Kyberd, D. Leggat, D. Leslie, W. Martin, I.D. Reid, P. Symonds, L. Teodorescu, M. Turner

Baylor University, Waco, USA

K. Hatakeyama, H. Liu, T. Scarborough

The University of Alabama, Tuscaloosa, USA

O. Charaf, C. Henderson, P. Rumerio

Boston University, Boston, USA

A. Avetisyan, T. Bose, C. Fantasia, A. Heister, J.St. John, P. Lawson, D. Lazic, J. Rohlf, D. Sperka, L. Sulak

Brown University, Providence, USA

J. Alimena, S. Bhattacharya, D. Cutts, A. Ferapontov, U. Heintz, S. Jabeen, G. Kukartsev, E. Laird, G. Landsberg, M. Luk, M. Narain, D. Nguyen, M. Segala, T. Sinthuprasith, T. Speer, K.V. Tsang

University of California, Davis, Davis, USA

R. Breedon, G. Breto, M. Calderon De La Barca Sanchez, S. Chauhan, M. Chertok, J. Conway, R. Conway, P.T. Cox, J. Dolen, R. Erbacher, M. Gardner, R. Houtz, W. Ko, A. Kopecky, R. Lander, T. Miceli, D. Pellett, F. Ricci-tam, B. Rutherford, M. Searle, J. Smith, M. Squires, M. Tripathi, R. Vasquez Sierra

University of California, Los Angeles, Los Angeles, USA

V. Andreev, D. Cline, R. Cousins, J. Duris, S. Erhan, P. Everaerts, C. Farrell, J. Hauser, M. Ignatenko, C. Jarvis, C. Plager, G. Rakness, P. Schlein[†], P. Traczyk, V. Valuev, M. Weber

University of California, Riverside, Riverside, USA

J. Babb, R. Clare, M.E. Dinardo, J. Ellison, J.W. Gary, F. Giordano, G. Hanson, G.Y. Jeng⁵⁰, H. Liu, O.R. Long, A. Luthra, H. Nguyen, S. Paramesvaran, J. Sturdy, S. Sumowidagdo, R. Wilken, S. Wimpenny

University of California, San Diego, La Jolla, USA

W. Andrews, J.G. Branson, G.B. Cerati, S. Cittolin, D. Evans, F. Golf, A. Holzner, R. Kelley, M. Lebourgeois, J. Letts, I. Macneill, B. Mangano, S. Padhi, C. Palmer, G. Petrucciani, M. Pieri, M. Sani, V. Sharma, S. Simon, E. Sudano, M. Tadel, Y. Tu, A. Vartak, S. Wasserbaech⁵¹, F. Würthwein, A. Yagil, J. Yoo

University of California, Santa Barbara, Santa Barbara, USA

D. Barge, R. Bellan, C. Campagnari, M. D'Alfonso, T. Danielson, K. Flowers, P. Geffert, J. Incandela, C. Justus, P. Kalavase, S.A. Koay, D. Kovalskyi, V. Krutelyov, S. Lowette, N. Mccoll, V. Pavlunin, F. Rebassoo, J. Ribnik, J. Richman, R. Rossin, D. Stuart, W. To, C. West

California Institute of Technology, Pasadena, USA

A. Apresyan, A. Bornheim, Y. Chen, E. Di Marco, J. Duarte, M. Gataullin, Y. Ma, A. Mott, H.B. Newman, C. Rogan, M. Spiropulu, V. Timciuc, J. Veverka, R. Wilkinson, S. Xie, Y. Yang, R.Y. Zhu

Carnegie Mellon University, Pittsburgh, USA

B. Akgun, V. Azzolini, A. Calamba, R. Carroll, T. Ferguson, Y. Iiyama, D.W. Jang, Y.F. Liu, M. Paulini, H. Vogel, I. Vorobiev

University of Colorado at Boulder, Boulder, USA

J.P. Cumalat, B.R. Drell, C.J. Edelmaier, W.T. Ford, A. Gaz, B. Heyburn, E. Luiggi Lopez, J.G. Smith, K. Stenson, K.A. Ulmer, S.R. Wagner

Cornell University, Ithaca, USA

J. Alexander, A. Chatterjee, N. Eggert, L.K. Gibbons, B. Heltsley, A. Khukhunaishvili, B. Kreis, N. Mirman, G. Nicolas Kaufman, J.R. Patterson, A. Ryd, E. Salvati, W. Sun, W.D. Teo, J. Thom, J. Thompson, J. Tucker, J. Vaughan, Y. Weng, L. Winstrom, P. Wittich

Fairfield University, Fairfield, USA

D. Winn

Fermi National Accelerator Laboratory, Batavia, USA

S. Abdullin, M. Albrow, J. Anderson, L.A.T. Bauerdick, A. Beretvas, J. Berryhill, P.C. Bhat, I. Bloch, K. Burkett, J.N. Butler, V. Chetluru, H.W.K. Cheung, F. Chlebana, V.D. Elvira, I. Fisk, J. Freeman, Y. Gao, D. Green, O. Gutsche, J. Hanlon, R.M. Harris, J. Hirschauer, B. Hooberman, S. Jindariani, M. Johnson, U. Joshi, B. Kilminster, B. Klima, S. Kunori, S. Kwan, C. Leonidopoulos, J. Linacre, D. Lincoln, R. Lipton, J. Lykken, K. Maeshima, J.M. Marraffino, S. Maruyama, D. Mason, P. McBride, K. Mishra, S. Mrenna, Y. Musienko⁵², C. Newman-Holmes, V. O'Dell, O. Prokofyev, E. Sexton-Kennedy, S. Sharma, W.J. Spalding, L. Spiegel, P. Tan, L. Taylor, S. Tkaczyk, N.V. Tran, L. Uplegger, E.W. Vaandering, R. Vidal, J. Whitmore, W. Wu, F. Yang, F. Yumiceva, J.C. Yun

University of Florida, Gainesville, USA

D. Acosta, P. Avery, D. Bourilkov, M. Chen, T. Cheng, S. Das, M. De Gruttola, G.P. Di Giovanni, D. Dobur, A. Drozdetskiy, R.D. Field, M. Fisher, Y. Fu, I.K. Furic, J. Gartner, J. Hugon, B. Kim, J. Konigsberg, A. Korytov, A. Kropivnitskaya, T. Kypreos, J.F. Low, K. Matchev, P. Milenovic⁵³, G. Mitselmakher, L. Muniz, R. Remington, A. Rinkevicius, P. Sellers, N. Skhirtladze, M. Snowball, J. Yelton, M. Zakaria

Florida International University, Miami, USA

V. Gaultney, S. Hewamanage, L.M. Lebolo, S. Linn, P. Markowitz, G. Martinez, J.L. Rodriguez

Florida State University, Tallahassee, USA

T. Adams, A. Askew, J. Bochenek, J. Chen, B. Diamond, S.V. Gleyzer, J. Haas, S. Hagopian, V. Hagopian, M. Jenkins, K.F. Johnson, H. Prosper, V. Veeraraghavan, M. Weinberg

Florida Institute of Technology, Melbourne, USA

M.M. Baarmand, B. Dorney, M. Hohlmann, H. Kalakhety, I. Vodopiyanov

University of Illinois at Chicago (UIC), Chicago, USA

M.R. Adams, I.M. Anghel, L. Apanasevich, Y. Bai, V.E. Bazterra, R.R. Betts, I. Bucinskaite, J. Callner, R. Cavanaugh, O. Evdokimov, L. Gauthier, C.E. Gerber, D.J. Hofman, S. Khalatyan, F. Lacroix, M. Malek, C. O'Brien, C. Silkworth, D. Strom, P. Turner, N. Varelas

The University of Iowa, Iowa City, USA

U. Akgun, E.A. Albayrak, B. Bilki⁵⁴, W. Clarida, F. Duru, S. Griffiths, J.-P. Merlo, H. Mermerkaya⁵⁵, A. Mestvirishvili, A. Moeller, J. Nachtman, C.R. Newsom, E. Norbeck, Y. Onel, F. Ozok, S. Sen, E. Tiras, J. Wetzel, T. Yetkin, K. Yi

Johns Hopkins University, Baltimore, USA

B.A. Barnett, B. Blumenfeld, S. Bolognesi, D. Fehling, G. Giurgiu, A.V. Gritsan, Z.J. Guo, G. Hu, P. Maksimovic, S. Rappoccio, M. Swartz, A. Whitbeck

The University of Kansas, Lawrence, USA

P. Baringer, A. Bean, G. Benelli, O. Grachov, R.P. Kenny Iii, M. Murray, D. Noonan, S. Sanders, R. Stringer, G. Tinti, J.S. Wood, V. Zhukova

Kansas State University, Manhattan, USA

A.F. Barfuss, T. Bolton, I. Chakaberia, A. Ivanov, S. Khalil, M. Makouski, Y. Maravin, S. Shrestha, I. Svintradze

Lawrence Livermore National Laboratory, Livermore, USA

J. Gronberg, D. Lange, D. Wright

University of Maryland, College Park, USA

A. Baden, M. Boutemur, B. Calvert, S.C. Eno, J.A. Gomez, N.J. Hadley, R.G. Kellogg, M. Kirn, T. Kolberg, Y. Lu, M. Marionneau, A.C. Mignerey, K. Pedro, A. Peterman, A. Skuja, J. Temple, M.B. Tonjes, S.C. Tonwar, E. Twedt

Massachusetts Institute of Technology, Cambridge, USA

A. Apyan, G. Bauer, J. Bendavid, W. Busza, E. Butz, I.A. Cali, M. Chan, V. Dutta, G. Gomez Ceballos, M. Goncharov, K.A. Hahn, Y. Kim, M. Klute, K. Krajczar⁵⁶, W. Li, P.D. Luckey, T. Ma, S. Nahn, C. Paus, D. Ralph, C. Roland, G. Roland, M. Rudolph, G.S.F. Stephans, F. Stöckli, K. Sumorok, K. Sung, D. Velicanu, E.A. Wenger, R. Wolf, B. Wyslouch, M. Yang, Y. Yilmaz, A.S. Yoon, M. Zanetti

University of Minnesota, Minneapolis, USA

S.I. Cooper, B. Dahmes, A. De Benedetti, G. Franzoni, A. Gude, S.C. Kao, K. Klapoetke, Y. Kubota, J. Mans, N. Pastika, R. Rusack, M. Sasseville, A. Singovsky, N. Tambe, J. Turkewitz

University of Mississippi, Oxford, USA

L.M. Cremaldi, R. Kroeger, L. Perera, R. Rahmat, D.A. Sanders

University of Nebraska-Lincoln, Lincoln, USA

E. Avdeeva, K. Bloom, S. Bose, J. Butt, D.R. Claes, A. Dominguez, M. Eads, J. Keller, I. Kravchenko, J. Lazo-Flores, H. Malbouissou, S. Malik, G.R. Snow

State University of New York at Buffalo, Buffalo, USA

U. Baur, A. Godshalk, I. Iashvili, S. Jain, A. Kharchilava, A. Kumar, S.P. Shipkowski, K. Smith

Northeastern University, Boston, USA

G. Alverson, E. Barberis, D. Baumgartel, M. Chasco, J. Haley, D. Nash, D. Trocino, D. Wood, J. Zhang

Northwestern University, Evanston, USA

A. Anastassov, A. Kubik, N. Mucia, N. Odell, R.A. Ofierzynski, B. Pollack, A. Pozdnyakov, M. Schmitt, S. Stoynev, M. Velasco, S. Won

University of Notre Dame, Notre Dame, USA

L. Antonelli, D. Berry, A. Brinkerhoff, M. Hildreth, C. Jessop, D.J. Karmgard, J. Kolb, K. Lannon, W. Luo, S. Lynch, N. Marinelli, D.M. Morse, T. Pearson, M. Planer, R. Ruchti, J. Slaunwhite, N. Valls, M. Wayne, M. Wolf

The Ohio State University, Columbus, USA

B. Bylsma, L.S. Durkin, C. Hill, R. Hughes, K. Kotov, T.Y. Ling, D. Puigh, M. Rodenburg, C. Vuosalo, G. Williams, B.L. Winer

Princeton University, Princeton, USA

N. Adam, E. Berry, P. Elmer, D. Gerbaudo, V. Halyo, P. Hebda, J. Hegeman, A. Hunt, P. Jindal, D. Lopes Pegna, P. Lujan, D. Marlow, T. Medvedeva, M. Mooney, J. Olsen, P. Piroué, X. Quan, A. Raval, B. Safdi, H. Saka, D. Stickland, C. Tully, J.S. Werner, A. Zuranski

University of Puerto Rico, Mayaguez, USA

J.G. Acosta, E. Brownson, X.T. Huang, A. Lopez, H. Mendez, S. Oliveros, J.E. Ramirez Vargas, A. Zatserklyaniy

Purdue University, West Lafayette, USA

E. Alagoz, V.E. Barnes, D. Benedetti, G. Bolla, D. Bortoletto, M. De Mattia, A. Everett, Z. Hu, M. Jones, O. Koybasi, M. Kress, A.T. Laasanen, N. Leonardo, V. Maroussov, P. Merkel, D.H. Miller, N. Neumeister, I. Shipsey, D. Silvers, A. Svyatkovskiy, M. Vidal Marono, H.D. Yoo, J. Zablocki, Y. Zheng

Purdue University Calumet, Hammond, USA

S. Guragain, N. Parashar

Rice University, Houston, USA

A. Adair, C. Boulahouache, K.M. Ecklund, F.J.M. Geurts, B.P. Padley, R. Redjimi, J. Roberts, J. Zabel

University of Rochester, Rochester, USA

B. Betchart, A. Bodek, Y.S. Chung, R. Covarelli, P. de Barbaro, R. Demina, Y. Eshaq, T. Ferbel, A. Garcia-Bellido, P. Goldenzweig, J. Han, A. Harel, D.C. Miner, D. Vishnevskiy, M. Zielinski

The Rockefeller University, New York, USA

A. Bhatti, R. Ciesielski, L. Demortier, K. Goulios, G. Lungu, S. Malik, C. Mesropian

Rutgers the State University of New Jersey, Piscataway, USA

S. Arora, A. Barker, J.P. Chou, C. Contreras-Campana, E. Contreras-Campana, D. Duggan, D. Ferencek, Y. Gershtein, R. Gray, E. Halkiadakis, D. Hidas, A. Lath, S. Panwalkar, M. Park, R. Patel, V. Rekovic, J. Robles, K. Rose, S. Salur, S. Schnetzer, C. Seitz, S. Somalwar, R. Stone, S. Thomas

University of Tennessee, Knoxville, USA

G. Cerizza, M. Hollingsworth, S. Spanier, Z.C. Yang, A. York

Texas A&M University, College Station, USA

R. Eusebi, W. Flanagan, J. Gilmore, T. Kamon⁵⁷, V. Khotilovich, R. Montalvo, I. Osipenkov, Y. Pakhotin, A. Perloff, J. Roe, A. Safonov, T. Sakuma, S. Sengupta, I. Suarez, A. Tatarinov, D. Toback

Texas Tech University, Lubbock, USA

N. Akchurin, J. Damgov, C. Dragoiu, P.R. Duderod, C. Jeong, K. Kovitanggoon, S.W. Lee, T. Libeiro, Y. Roh, I. Volobouev

Vanderbilt University, Nashville, USA

E. Appelt, A.G. Delannoy, C. Florez, S. Greene, A. Gurrola, W. Johns, C. Johnston, P. Kurt, C. Maguire, A. Melo, M. Sharma, P. Sheldon, B. Snook, S. Tuo, J. Velkovska

University of Virginia, Charlottesville, USA

M.W. Arenton, M. Balazs, S. Boutle, B. Cox, B. Francis, J. Goodell, R. Hirosky, A. Ledovskoy, C. Lin, C. Neu, J. Wood, R. Yohay

Wayne State University, Detroit, USA

S. Gollapinni, R. Harr, P.E. Karchin, C. Kottachchi Kankanamge Don, P. Lamichhane, A. Sakharov

University of Wisconsin, Madison, USA

M. Anderson, D. Belknap, L. Borrello, D. Carlsmith, M. Cepeda, S. Dasu, E. Friis, L. Gray, K.S. Grogg, M. Grothe, R. Hall-Wilton, M. Herndon, A. Hervé, P. Klabbbers, J. Klukas, A. Lanaro, C. Lazaridis, J. Leonard, R. Loveless, A. Mohapatra, I. Ojalvo, F. Palmonari, G.A. Pierro, I. Ross, A. Savin, W.H. Smith, J. Swanson

†: Deceased

- 1: Also at Vienna University of Technology, Vienna, Austria
- 2: Also at National Institute of Chemical Physics and Biophysics, Tallinn, Estonia
- 3: Also at Universidade Federal do ABC, Santo Andre, Brazil
- 4: Also at California Institute of Technology, Pasadena, USA
- 5: Also at CERN, European Organization for Nuclear Research, Geneva, Switzerland
- 6: Also at Laboratoire Leprince-Ringuet, Ecole Polytechnique, IN2P3-CNRS, Palaiseau, France
- 7: Also at Suez Canal University, Suez, Egypt
- 8: Also at Zewail City of Science and Technology, Zewail, Egypt
- 9: Also at Cairo University, Cairo, Egypt
- 10: Also at Fayoum University, El-Fayoum, Egypt
- 11: Also at British University, Cairo, Egypt
- 12: Now at Ain Shams University, Cairo, Egypt
- 13: Also at National Centre for Nuclear Research, Swierk, Poland
- 14: Also at Université de Haute-Alsace, Mulhouse, France
- 15: Now at Joint Institute for Nuclear Research, Dubna, Russia
- 16: Also at Moscow State University, Moscow, Russia
- 17: Also at Brandenburg University of Technology, Cottbus, Germany
- 18: Also at Institute of Nuclear Research ATOMKI, Debrecen, Hungary
- 19: Also at Eötvös Loránd University, Budapest, Hungary
- 20: Also at Tata Institute of Fundamental Research - HECR, Mumbai, India
- 21: Also at University of Visva-Bharati, Santiniketan, India
- 22: Also at Sharif University of Technology, Tehran, Iran
- 23: Also at Isfahan University of Technology, Isfahan, Iran
- 24: Also at Plasma Physics Research Center, Science and Research Branch, Islamic Azad University, Tehran, Iran
- 25: Also at Facoltà Ingegneria Università di Roma, Roma, Italy

- 26: Also at Università della Basilicata, Potenza, Italy
- 27: Also at Università degli Studi Guglielmo Marconi, Roma, Italy
- 28: Also at Università degli Studi di Siena, Siena, Italy
- 29: Also at University of Bucharest, Faculty of Physics, Bucuresti-Magurele, Romania
- 30: Also at Faculty of Physics of University of Belgrade, Belgrade, Serbia
- 31: Also at University of California, Los Angeles, Los Angeles, USA
- 32: Also at Scuola Normale e Sezione dell' INFN, Pisa, Italy
- 33: Also at INFN Sezione di Roma; Università di Roma, Roma, Italy
- 34: Also at University of Athens, Athens, Greece
- 35: Also at Rutherford Appleton Laboratory, Didcot, United Kingdom
- 36: Also at The University of Kansas, Lawrence, USA
- 37: Also at Paul Scherrer Institut, Villigen, Switzerland
- 38: Also at Institute for Theoretical and Experimental Physics, Moscow, Russia
- 39: Also at Gaziosmanpasa University, Tokat, Turkey
- 40: Also at Adiyaman University, Adiyaman, Turkey
- 41: Also at Izmir Institute of Technology, Izmir, Turkey
- 42: Also at The University of Iowa, Iowa City, USA
- 43: Also at Mersin University, Mersin, Turkey
- 44: Also at Ozyegin University, Istanbul, Turkey
- 45: Also at Kafkas University, Kars, Turkey
- 46: Also at Suleyman Demirel University, Isparta, Turkey
- 47: Also at Ege University, Izmir, Turkey
- 48: Also at School of Physics and Astronomy, University of Southampton, Southampton, United Kingdom
- 49: Also at INFN Sezione di Perugia; Università di Perugia, Perugia, Italy
- 50: Also at University of Sydney, Sydney, Australia
- 51: Also at Utah Valley University, Orem, USA
- 52: Also at Institute for Nuclear Research, Moscow, Russia
- 53: Also at University of Belgrade, Faculty of Physics and Vinca Institute of Nuclear Sciences, Belgrade, Serbia
- 54: Also at Argonne National Laboratory, Argonne, USA
- 55: Also at Erzincan University, Erzincan, Turkey
- 56: Also at KFKI Research Institute for Particle and Nuclear Physics, Budapest, Hungary
- 57: Also at Kyungpook National University, Daegu, Korea